Exploring and Exploiting Rarefied Flows for Novel Microdevices

Alina Alexeenko
School of Aeronautics and Astronautics
Purdue University

UToronto – October 17, 2014

Applications of Rarefied Gas Dynamics

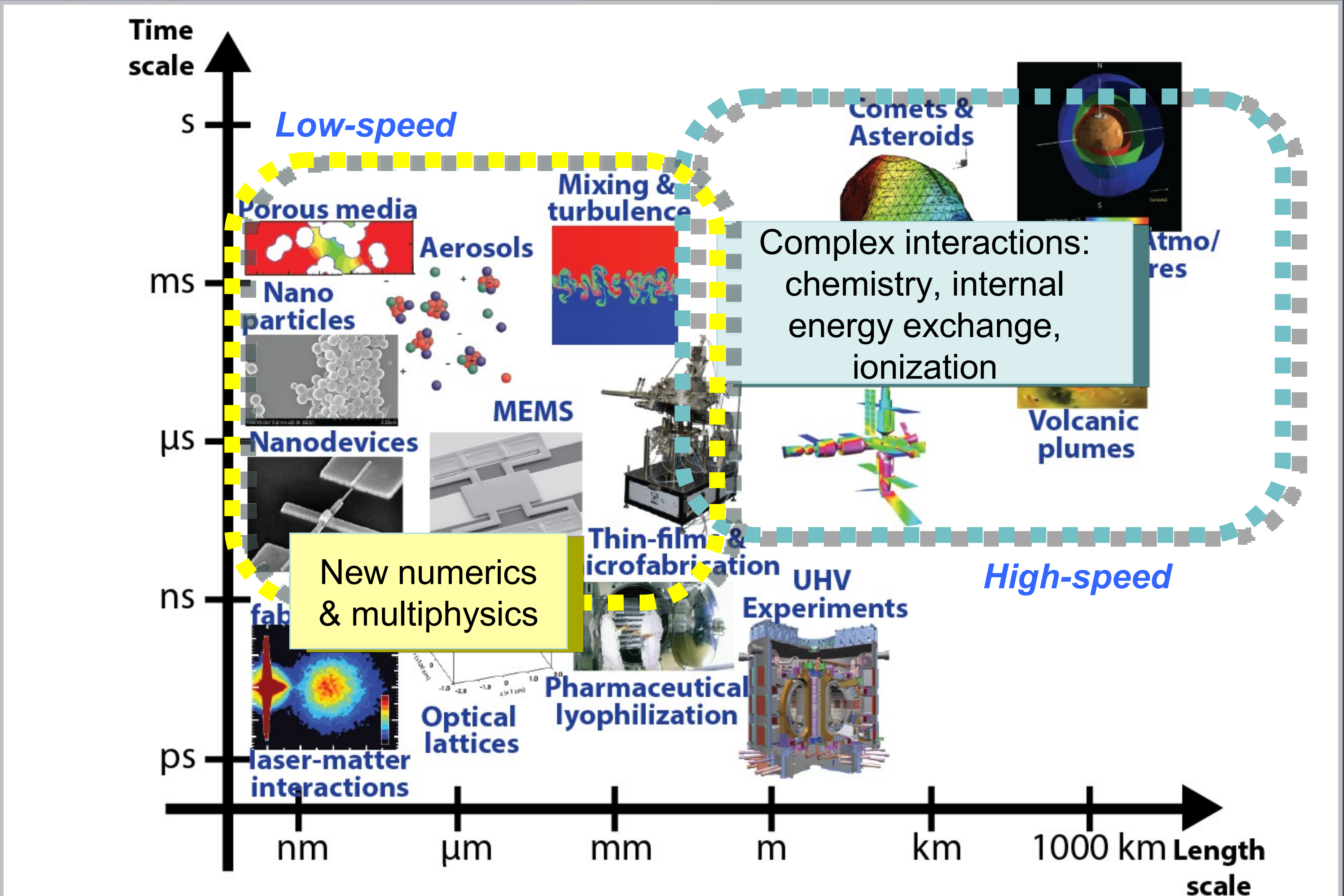

Outline

- Exploring low-speed microflows:
  - Deterministic methods for rarefied gas flows:
    - A-priori accuracy estimate: discrete H-theorem
    - FVM + Immersed boundary / cut-cell methods for moving boundaries
    - Discontinuous Galerkin methods
  - *Example*: understanding rarefied gas damping effects in RF MEMS switches by coupled fluid/structural/electrostatic analysis
- Exploiting microscale effects for microdevices:
  - ❑ Knudsen compressor for on-chip vacuum
  - ❑ Knudsen force actuation/sensing
  - ❑ Field-emission driven microdischarges

Gas-Based Microdevices

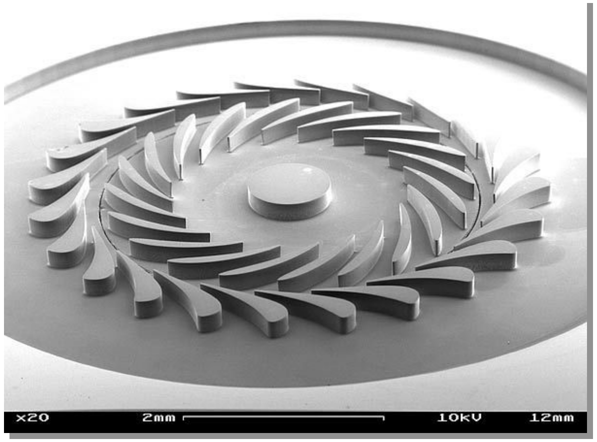

MIT micro-turbine

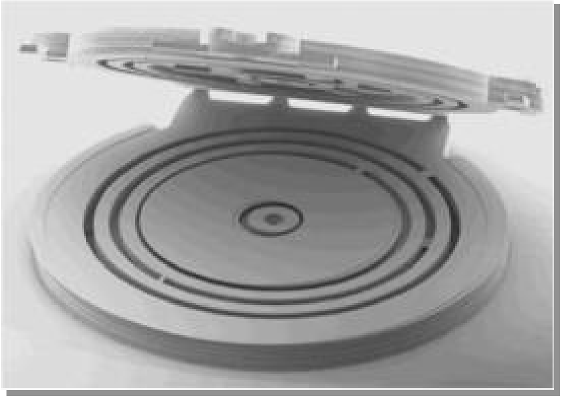

USC micro-burner

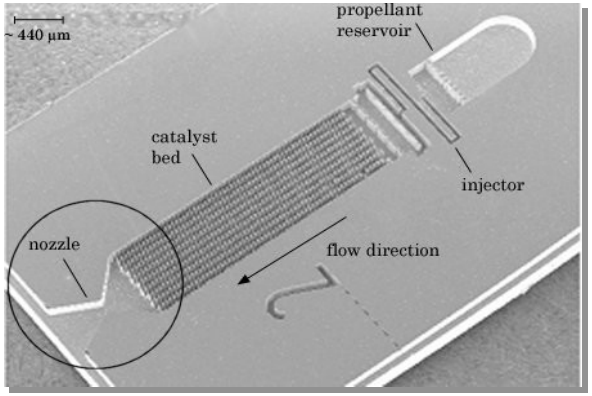

NASA/UVM micro-thruster

Microscale Challenges:

- Gas-phase extinction limit, min Re~40. Catalyst needed
- Amplified heat transfer losses
- Increased viscous losses: Isp drops for Re<200.

Rarefied flow analysis provides methods for design to overcome these challenges

Microdevices Exploiting Rarefied Flow

Vargo, Muntz , Shiflett, Tang, “Knudsen Compressor as a Micro/Meso-scale Vacuum Pump”, *JVST A*, 1999:

a cascade of multiple, individually heated compressor stages that exploit the pumping effect of rarefied thermal transpiration.

Vargo and Muntz (USC), 2001

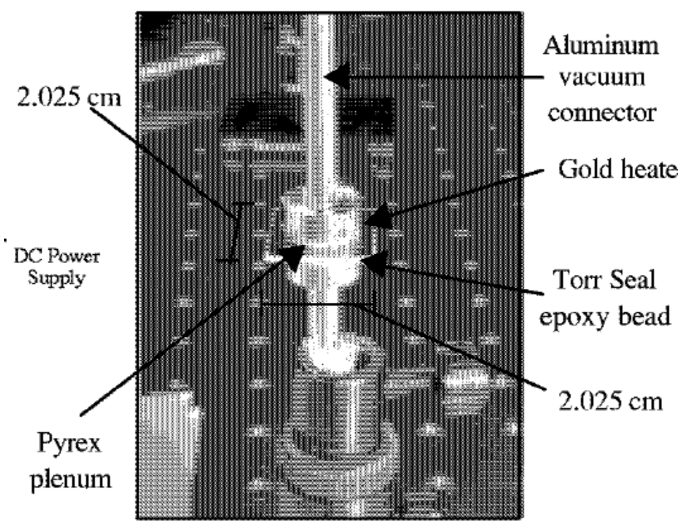

1-stage:
1.5 W, 2 cmx2cm
760 → 750 torr

McNamara&Gianchandani (UMich), 2003

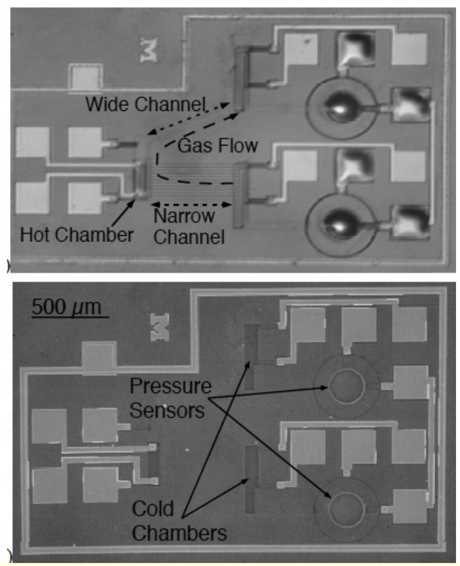

1-stage:
80 mW, 2 x 2 mm^2
760 → 350 torr

Gupta, Ann, Gianchandani (UMich), 2012

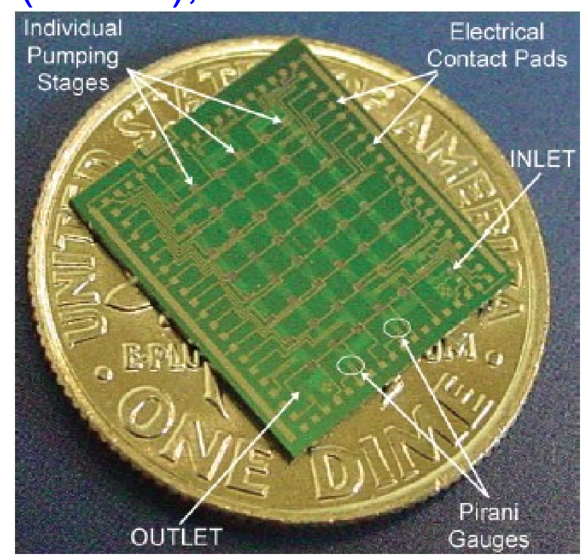

48-stage:
1350 mW, 1cm^2
760 → 50 or 250 → 5 torr

Numerical Modeling Approach: FVM

Unsteady Boltzmann model kinetic equation for velocity distribution function:

$$\frac{\partial f}{\partial t} + \vec{u} \cdot \nabla_{\vec{x}} f = \frac{1}{\tau}(f_0 - f)$$

•ESBGK collision operator

- H-theorem proved by Andries et al, 2000.
- Conservative discretization by perturbed Gaussian by Mieussens, *JPC*, 2000.

<u>FMV Solver:</u>

•Discrete ordinates in velocity space with Gauss-Hermite

•FVM in physical space with 3rd-order WENO fluxes.

•2nd and 3rd -order time integration with Runge-Kutta TVD schemes

•domain decomposition in physical space

Entropy Properties

Boltzmann's Entropy: $S=-k\ \ln(\Omega)$ $\quad S=k\int_{-\infty}^{\infty} f(\vec{c})\left[1-\ln\left(\frac{h^3 f(\vec{c})}{m^3}\right)\right]d\vec{c}$

Boltzmann's H-Theorem: $\dot{S}\geq 0$

High entropy generation rate as indicator of non-equilibrium (**Naterer & Camberos, *JTHT*, 2003**)

Entropy generation rate as moment of BE:

$$\dot{S}_{lhs}=\frac{\partial S}{\partial t}+\nabla.\left(k\int_{-\infty}^{\infty}\vec{c}f(\vec{c})\left[1-\ln\left(\frac{h^3 f(\vec{c})}{m^3}\right)\right]d\vec{c}\right)$$

$$\dot{S}_{coll}=-\nu\int_{-\infty}^{\infty}\left(f(\vec{c})-f_0(\vec{c})\right)\ln\left(\frac{h^3 f(\vec{c})}{m^3}\right)d\vec{c}$$

Entropy generation rate based on macro-parameters:

$$\dot{S}=\frac{\Phi}{T}+\frac{\kappa}{T^2}\nabla T^2 \qquad \Phi=\mu\left(\frac{2}{3}\left[\frac{\partial u}{\partial x}+\frac{\partial v}{\partial y}\right]^2+\frac{2}{3}\left(\frac{\partial u}{\partial x}-\frac{\partial v}{\partial y}\right)^2+\left(\frac{\partial u}{\partial y}+\frac{\partial v}{\partial x}\right)^2\right)$$

Accuracy Analysis: Discrete H-Theorem

Governing equation:

$$\frac{\partial f}{\partial t}+\vec{c}\cdot\frac{\partial f}{\partial \vec{x}}=\frac{f_0-f}{\tau}$$

Discrete equation:

$$L^t(f^{i,j})+L^x(f^{i,j})=\frac{f_0^{i,j}-f^{i,j}}{\tau^{i,j}}$$

Boltzmann's H-Theorem:

$$\dot{S}\geq 0$$

Discrete analog of H-Theorem:

$$\dot{S}_{\mathrm{lhs}}^{i,j}=L^t(S^{i,j})+L^x(\sum_j c_j f^{i,j}[1-\ln\left(\frac{h^3 f^{i,j}}{m^3}\right)]\delta c_j)$$

$$\dot{S}_{\mathrm{coll}}^{i,j}=-\nu\sum_j\left(f^{i,j}-f_0^{i,j}\right)\ln\left(\frac{h^3 f^{i,j}}{m^3}\right)\delta c_j$$

$$\boxed{\dot{S}_{lhs}^{i,j}=\dot{S}_{\mathrm{coll}}^{i,j}\geq 0}$$

Chigullapalli, Venkattraman, Ivanov, Alexeenko, *J. Comp. Phys,* 2010

Approach to equilibrium: 0D3V

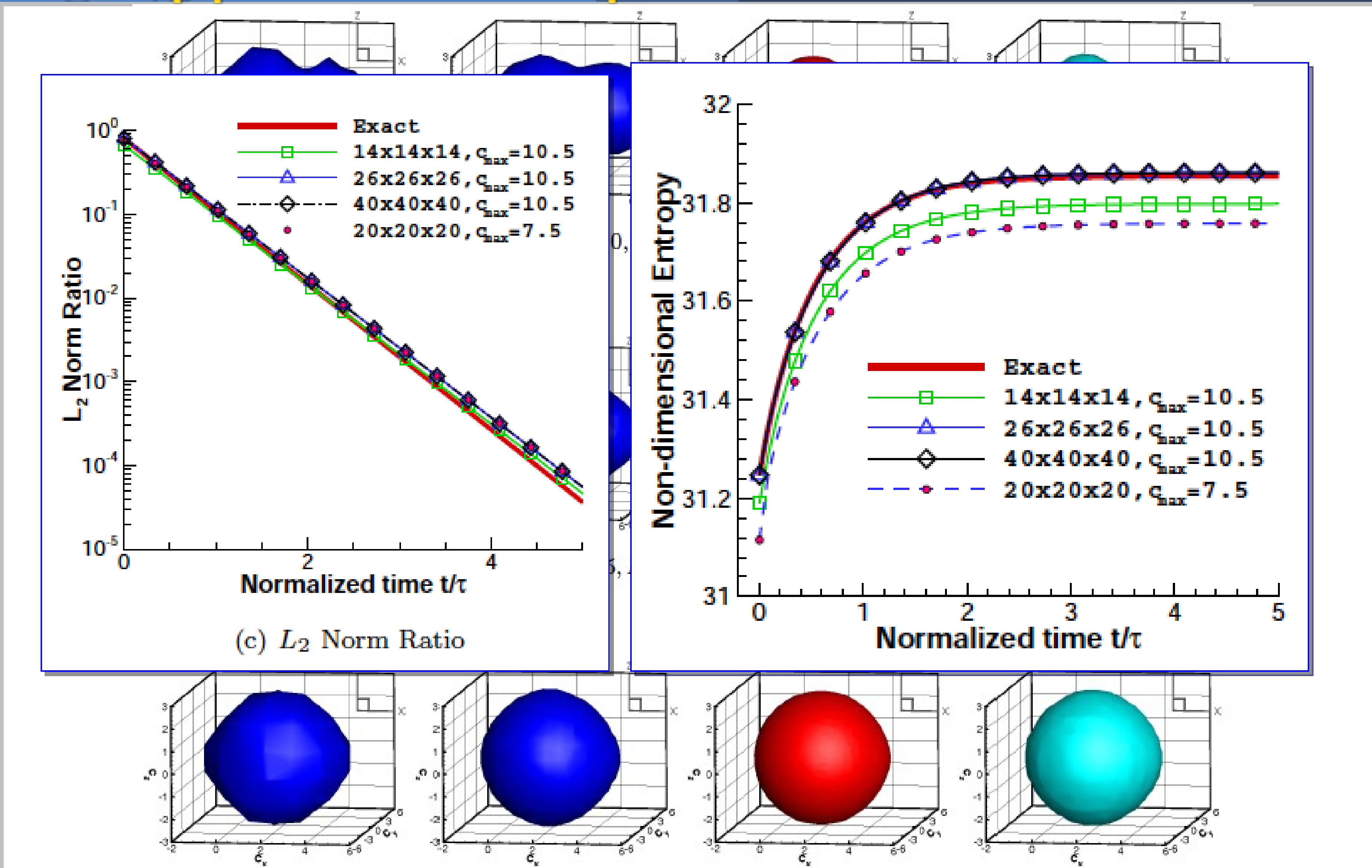

(c) L_2 Norm Ratio

(i) BGK, $\tilde{t} = 4.26, N = 14^3$

(j) BGK, $\tilde{t} = 4.26, N = 26^3$

(k) Exact, $\tilde{t} = 4.26$

(l) BGK, $\tilde{t} = 4.26, N = 20^3, c_{max} = 7.5$

1D3V Riemann Problem

1st order

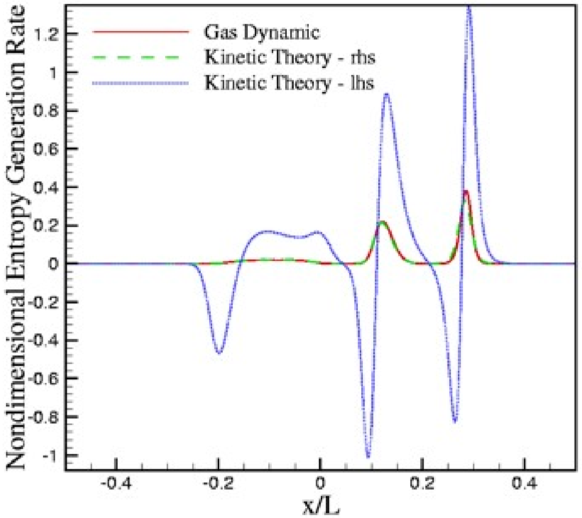

2nd order minmod

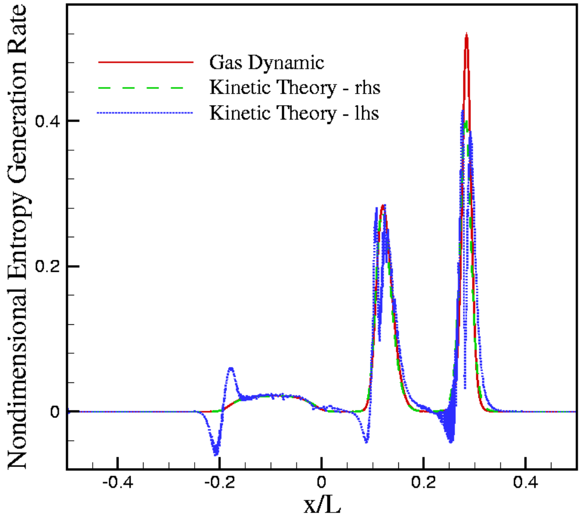

3rd order WENO

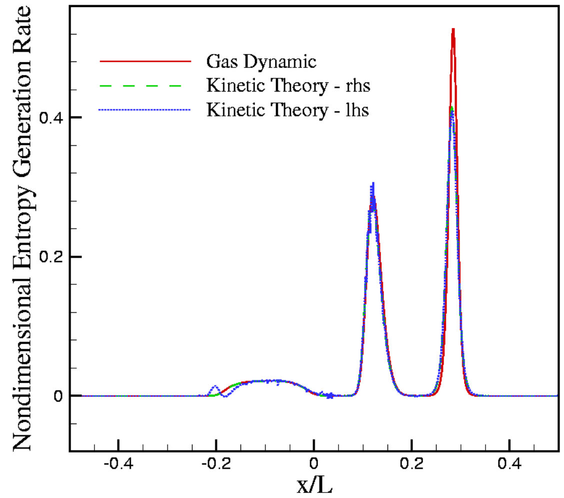

1001 x(40x20x10) mesh

- **Accuracy of numerical solution manifested in kinetic entropy generation rate.**
- **The entropy generation rate displays three peaks corresponding to the shock, contact discontinuity and the rarefaction wave.**

Chigullapalli, Venkattraman, Ivanov, Alexeenko, *J. Comp. Phys,* 2010

1D3V M=1.4 Normal Shock

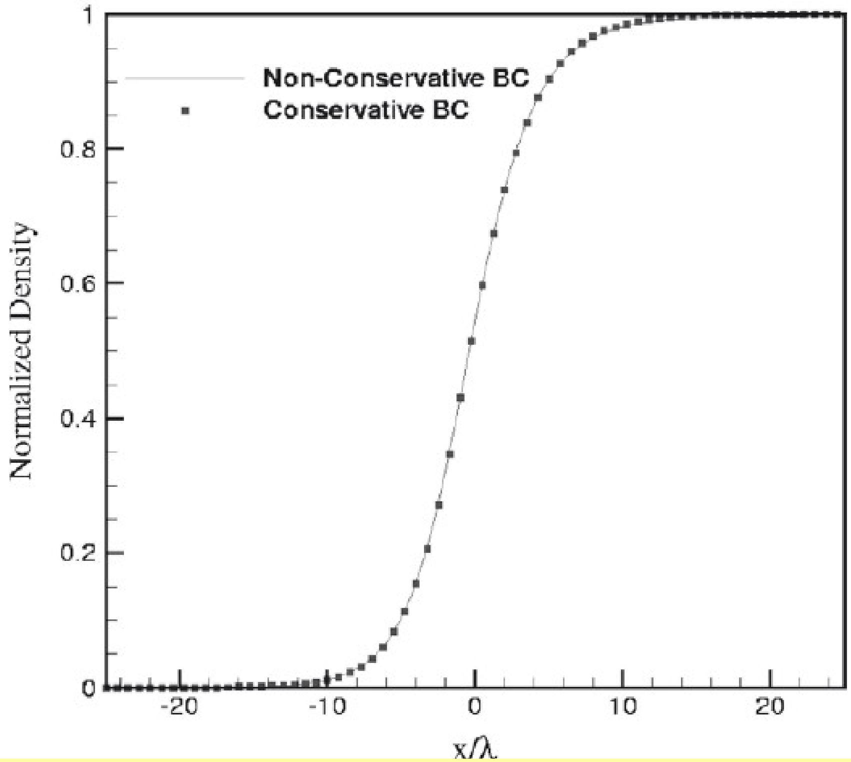

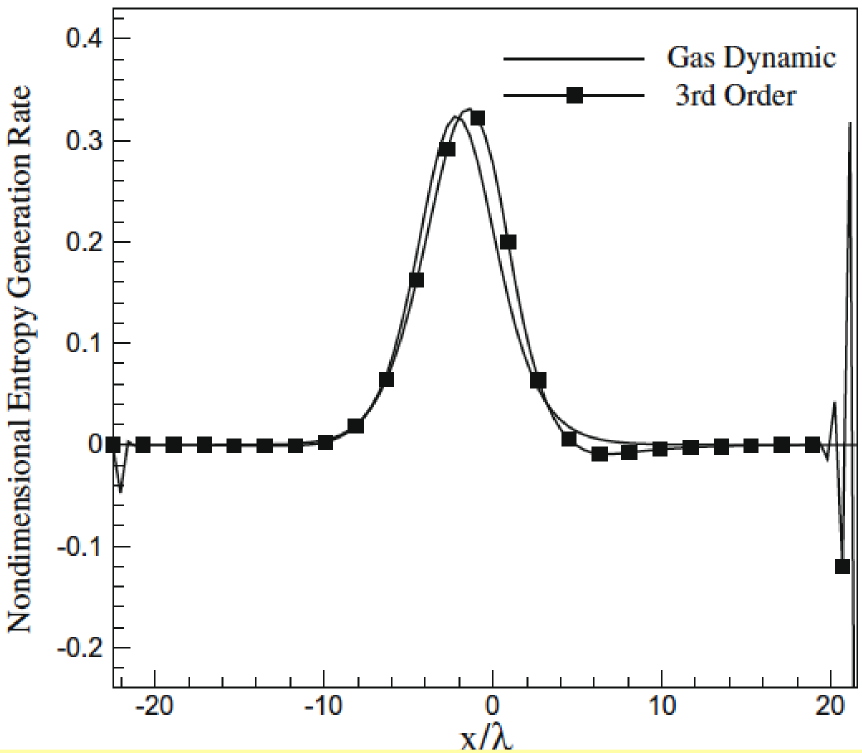

- **The entropy generation rate as indicator of compatibility of BC.**

Chigullapalli, Venkattraman, Ivanov, Alexeenko, *J. Comp. Phys,* 2010

IBM for Microflows: Motivation

High Frequency Micro Electro Mechanical Devices (MEMS)

Raman Group -Fluid structure interaction and nonlinear dynamics in RF-MEMS devices (part of the PRISM center for the prediction of reliability, integrability, and survivability of microsystems) Purdue University

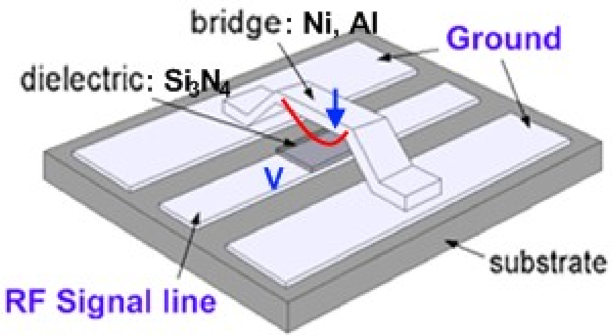

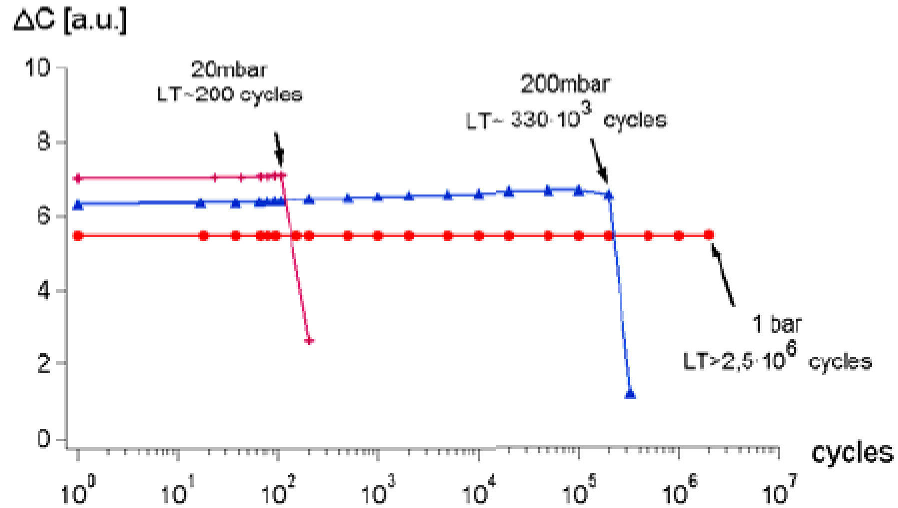

Lifetime of switches tested at 35 V and 100 Hz.

*Czarnecki et.al, 19th IEEE Conference on MEMS, 2006

IBM Formulations: Interpolation

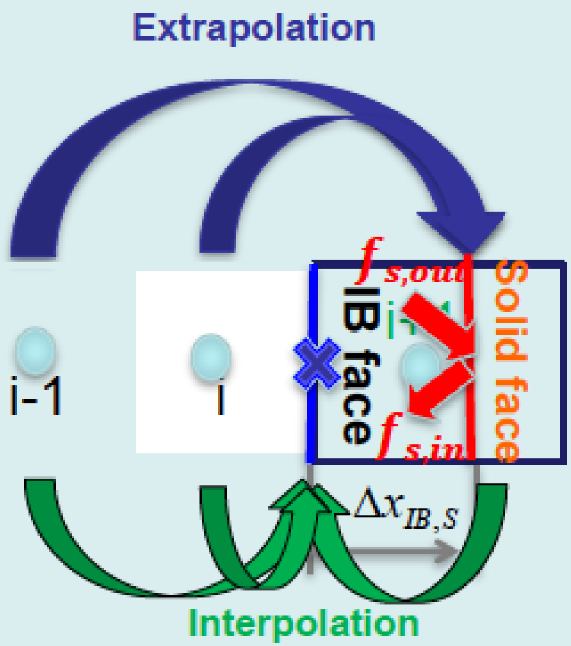

Step 1: Find $f_{outgoing}$ using 2nd order Least Squares Interpolation.

$$\emptyset = \beta_0 + \beta_1 x + \beta_1 x^2$$

$$M = \begin{pmatrix} 1 & x_1 & {x_1}^2 \\ 1 & x_2 & {x_2}^2 \\ \vdots & \vdots & \vdots \\ 1 & x_n & {x_n}^2 \end{pmatrix}$$

Minimize $\quad |\Phi - M\beta|^2$

Find $\quad \beta = (M^T M)^{-1} M^T\ \Phi$

Step 2: Conservation of mass flux at solid face

$$\sum_{\vec{c}.\vec{n}>0} \vec{c}.\vec{n} f_{s,out} + n_{wall} \sum_{\vec{c}.\vec{n}<0} \vec{c}.\vec{n} \exp\left(-\frac{(\vec{c}-\vec{v})^2}{T}\right) = 0$$

Step 3: Interpolate $f_{incoming}$ at IB face

Step 4: Solve $A\delta f+R=0$ for all directions

IBM Formulations: Relaxation

Step 1: Relax f_{IB} for each direction using

$$f_{s,out} = f_{\gamma,FCells} + (f_{IB,FCells} - f_{\gamma,FCells})\exp(\frac{-t}{\tau_{IB}})$$

$$t = \frac{\Delta x_{IB}}{\vec{c}\,.\vec{n}}$$ [Ref. 4,5]

Step 2: Conservation of mass flux at solid face centroid to find $f_{s,in}$

$$\sum_{\vec{c}.\vec{n}>0} \vec{c}.\vec{n} f_{s,out} + n_{wall} \sum_{\vec{c}.\vec{n}<0} \vec{c}.\vec{n}\exp(-\frac{(\vec{c}-\vec{v})^2}{T}) = 0$$

Step 3: Relax $f_{s,in}$ for each directions using

$$f_{IB,in} = f_{\gamma,IB} + (f_{s,out} - f_{\gamma,IB})\exp(\frac{-t}{\tau_{IB}})$$

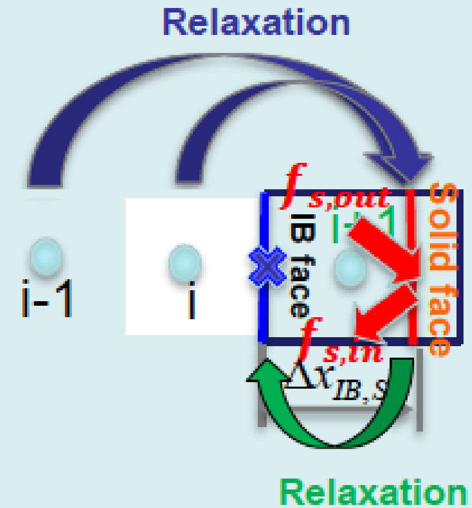

C.K. Chu Kinetic theoretic description of the formation of shock ware, Phys. Of Fluids, 8(1):12, 1965

Y. Ruan and A. Jameson, Gas-Kinetic BGK schemes for three-dimensional compressible flows, AIAA 2002-0550

IBM Fluxes: Interrelaxation

Step 1: Interpolate macroparameters and f at IB face using only interior values.

Step 2: Relax f_{IB} for each direction using

$$f_{s,out} = f_{\gamma,IB} + (f_{IB,out} - f_{\gamma,IB})\exp(\frac{-t}{\tau_{IB}}) \quad t = \frac{\Delta x_{IB}}{\vec{c}.\vec{n}}$$

Step 3: Conservation of mass flux at solid face centroid to find $f_{s,in}$

$$\sum_{\vec{c}.\vec{n}>0} \vec{c}.\vec{n} f_{s,out} + n_{wall} \sum_{\vec{c}.\vec{n}<0} \vec{c}.\vec{n}\exp(-\frac{(\vec{c}-\vec{v})^2}{T}) = 0$$

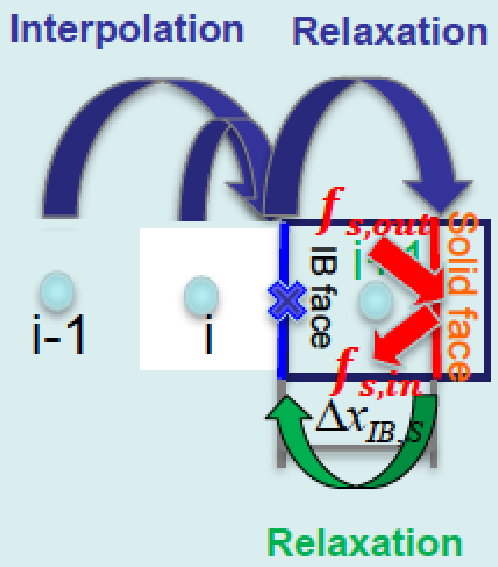

Step 4: Interpolate macroparameters at IB face using interior and solid values

Step 5: Relax $f_{s,in}$ for each j $\quad f_{IB,in} = f_{\gamma,IB} + (f_{s,out} - f_{\gamma,IB})\exp(\frac{-t}{\tau_{IB}})$

Error is less than 1% when $Kn_{\Delta x_{IB}} = \frac{\lambda}{\Delta x_{IB}} \geq 1.9$

IBM-ESBGK: 2D Verification

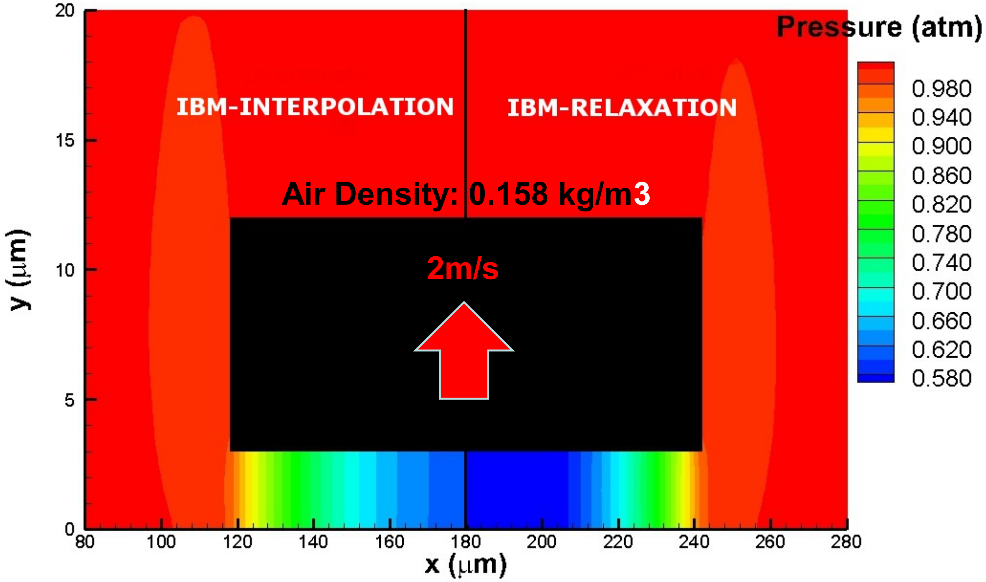

- ESBGK type collision approximation
- ESBGK-IB Methods are compared with ESBGK-FVM Solver
- Material Point Method Procedure is implemented for marking of background mesh
- Two different meshes having 10,800 and 20,100 elements are used
- A quadrature of 14x14x14 is used

$$Kn_{\Delta x_{IB} \min} = \frac{\lambda}{\Delta x_{IB}} = \infty \geq 1.9$$

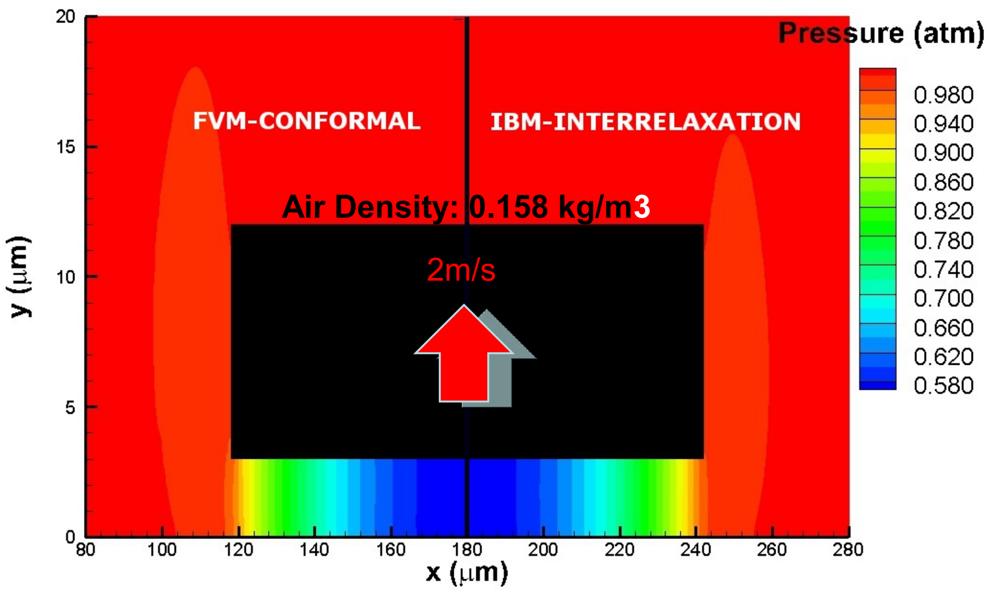

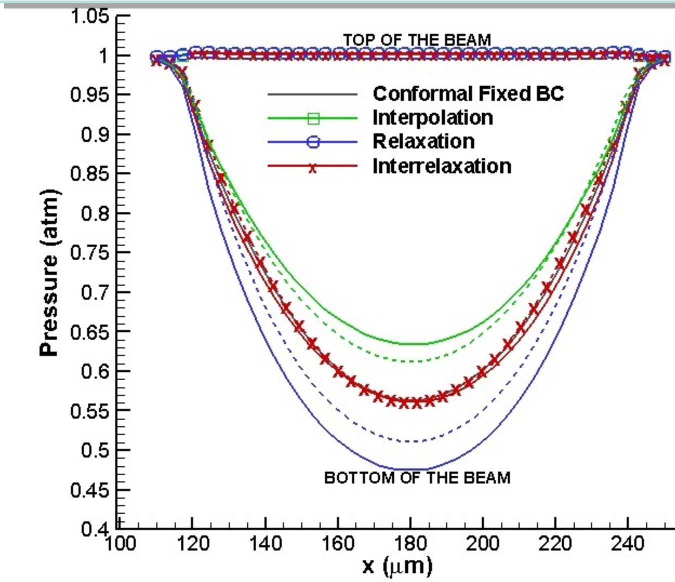

Solid - 10,800 cells; Dashed - 20,100 cells

IBM-ESBGK: Microbeam under 1E6 g

Temperature

Pressure

Δt= 6.25 ns

Max Velocity= 5.684 m/s

Width: 5 μm, **Width/Gap$_0$** = 2.5

Background mesh: 10,920 cells

Δx=0.1 μm, **Δy**=0.2 to 1 μm

IBM-ESBGK: Microbeam under 1E6 g

Time = 200 ns
Vbeam = 1.953 m/s

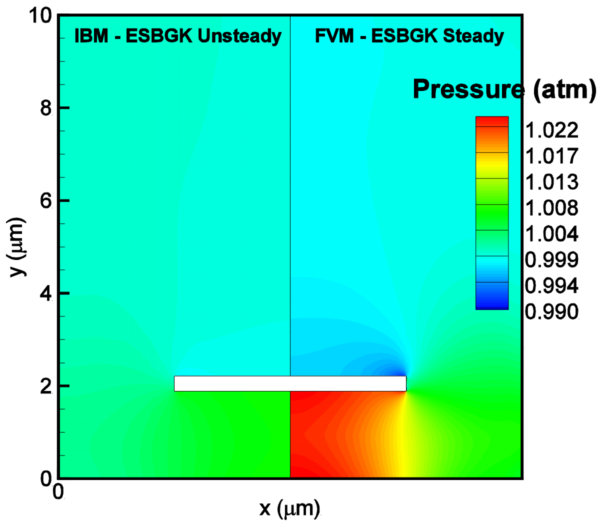

Time = 400 ns
Vbeam = 3.883 m/s

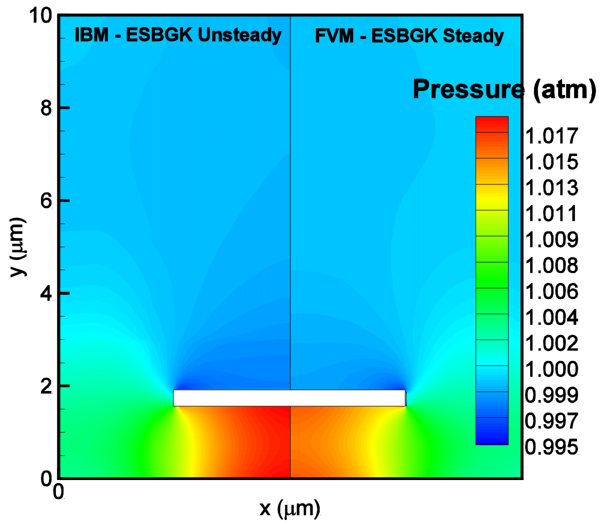

Time = 606 ns
Vbeam = 5.684 m/s

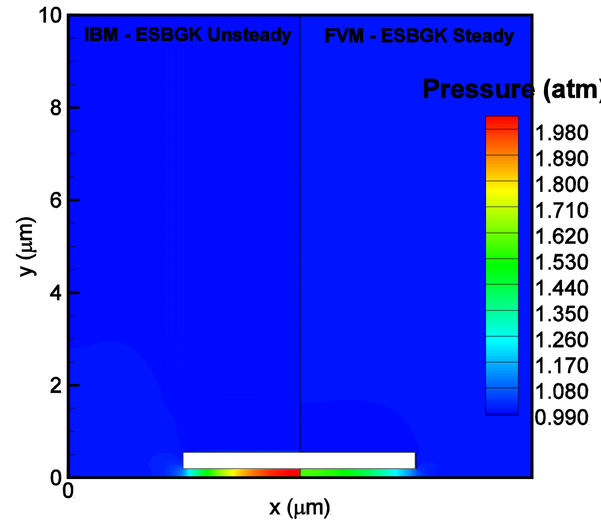

Width: 5 μm, **Width/Gap$_0$** = 2.5
Background mesh: 10,920 cells
Δx=0.1 μm, **Δy**=0.2 to 1 μm

3D3V Gas Damping in MEMS switch

Pressure and Streamlines for PRISM Gen5 Device during Pull-In

PRISMCG Online Tool

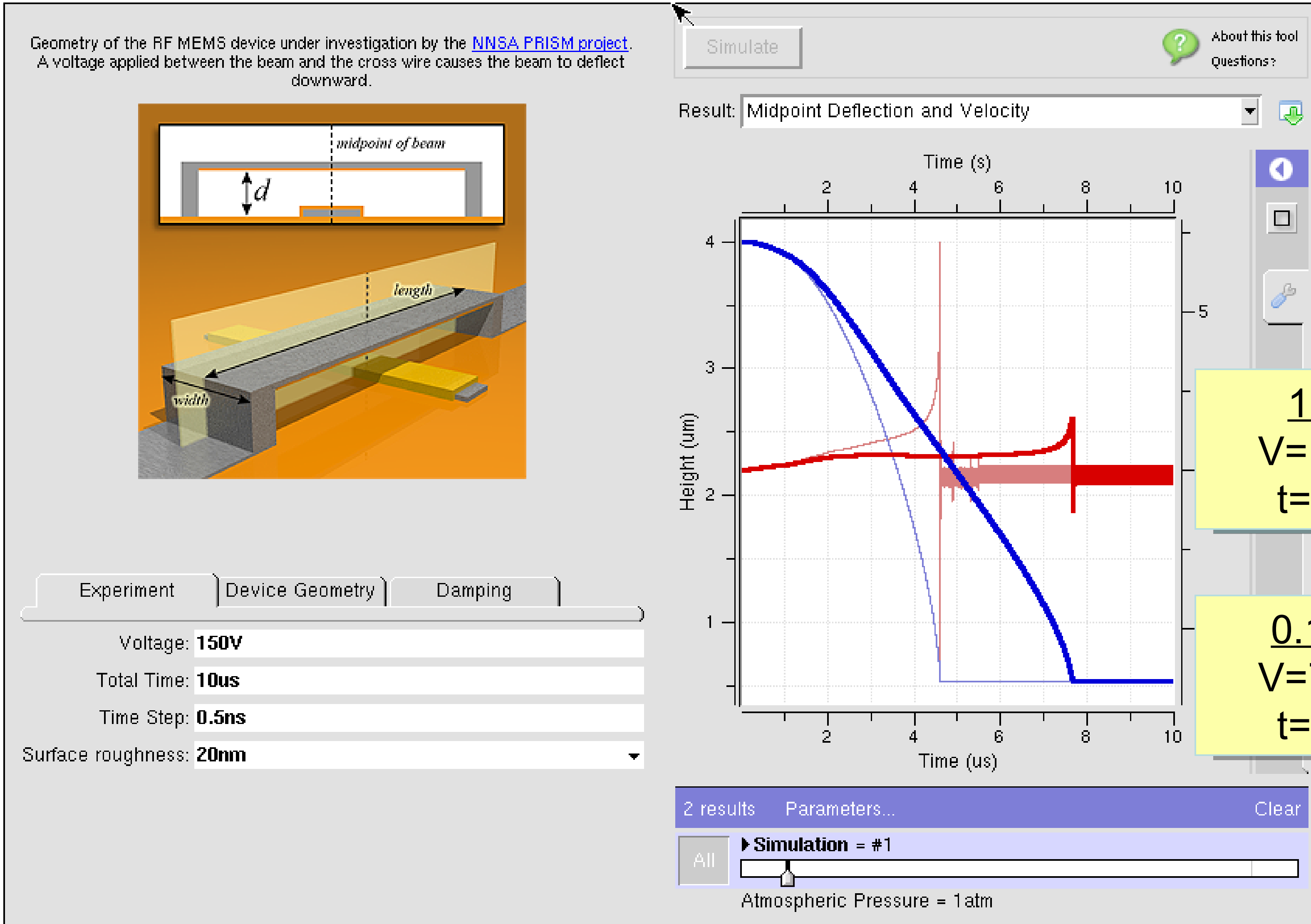

1 atm:
V=1.4 m/s
t=4.6 us

0.1 atm:
V=7.2 m/s
t=1.4 us

http://www.nanohub.org/tools/prismcg

Impulsive Effects in Switch Dynamics

PRISM device:

- L = 510 µm
- b = 122 µm
- t = 4µm
- td = 250 nm
- 1 atm air
- 150 V

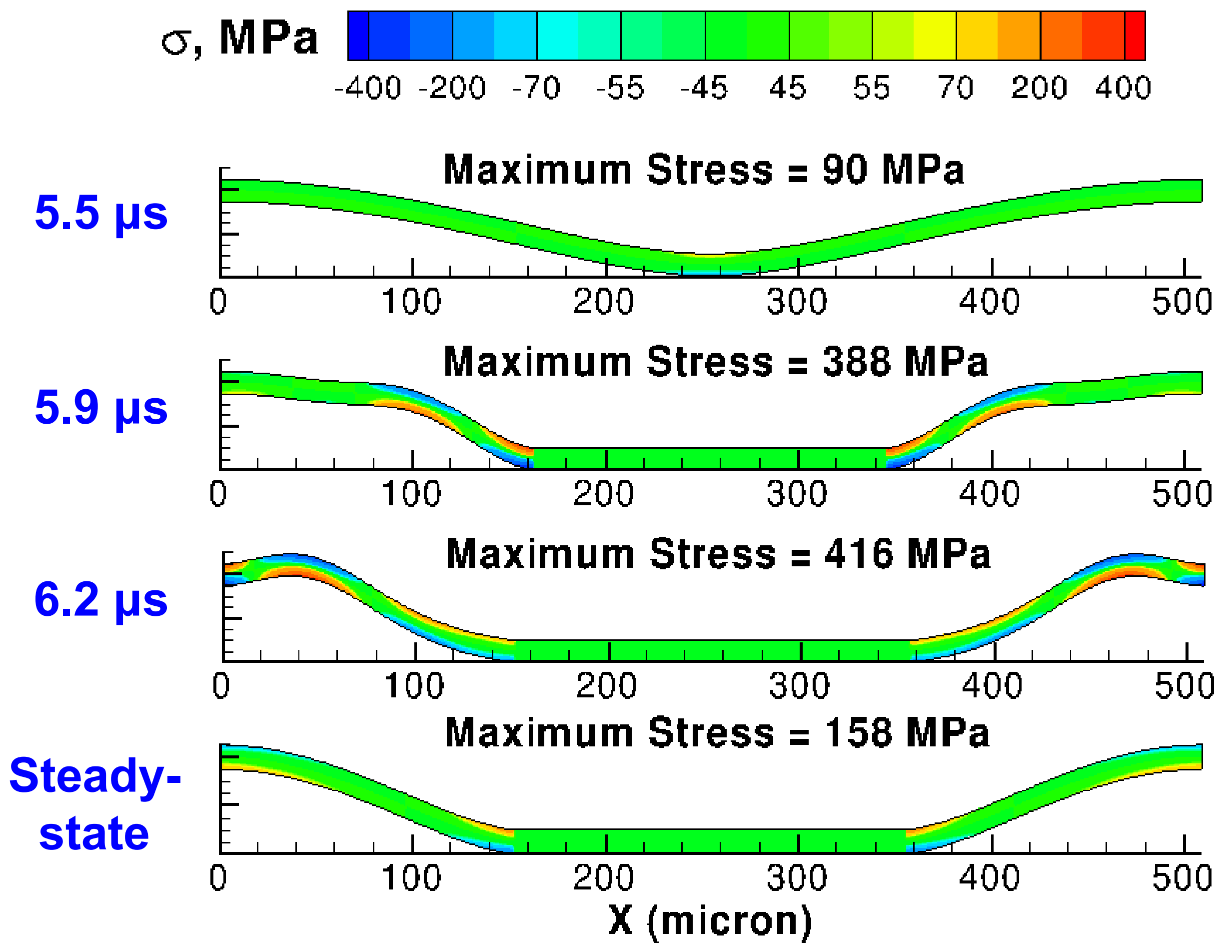

- Flexural wave reflection from boundaries lead to stresses which are higher by > 2.5x compared to static.

Impulsive Dynamics and Switch Lifetime

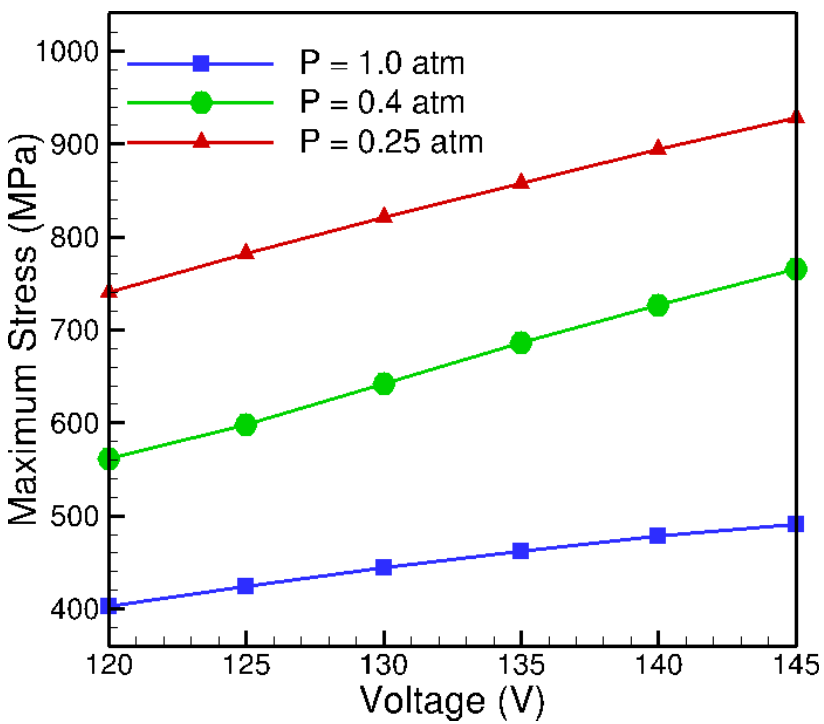

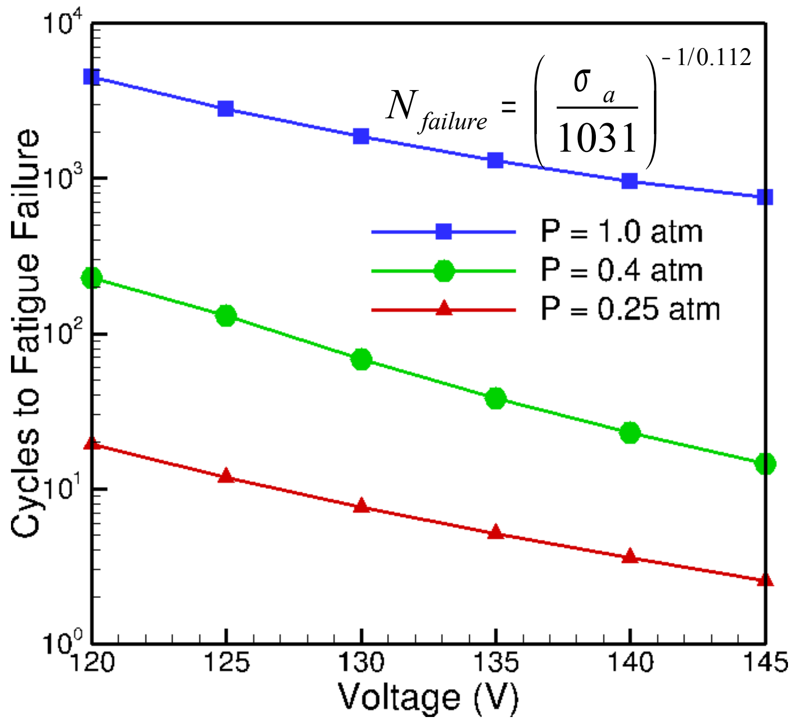

- The maximum bending stress in the beam for a given voltage increases with decreasing pressure.
- The maximum stress is converted to cycles to failure using a S-N relation* for typical LIGA Ni.

*** T.S. Slack, F. Sadhegi, and D. Peroulis, JMEMS, 2009***

High-Order Methods for Boltzmann-ESBGK

- **High-order deterministic methods**
  - Discretizations of Coordinate Space
    - Finite Difference Method & Finite Volume with high-order fluxes (i.e. WENO) Review by Luc Mieussens, RGD 2014.
    - High-order Finite Element / Discontinuous Galerkin methods

    Lesaint & Raviart, 1974
    - Spectral methods: work better on globally smooth functions

- **Advantages of Runge-Kutta discontinuous Galerkin method**
  - Very suitable for the solution of time-dependent hyperbolic and advection dominated advection-diffusion equations
  - naturally obtain fluxes at the boundaries with the same high-order accuracy as in the interior of the domain
  - Efficient parallel implementation due to compactness of the scheme

<u>Additional references:</u>

B. Cockburn and C. W. Shu. TVB Runge-Kutta local projection discontinuous Galerkin finite element method for scalar conservation laws IV: The multidimensional case. *Math. Comp.*, 54: 545-581,1990.
A. Alexeenko, C. Galitzine, A. M. Alekseenko, AIAA Paper 2008-4256
M. Alekseenko. Numerical properties of high order discrete velocity solutions of the BGK kinetic equation. *Applied Numerical Methermatics*, 61(4), 2011. pp 410-427
W. Su, A. Alexeenko, C. Cai, A Runge-Kutta discontinuous Galerkin solver for 2D Boltzmann model equations: Verification and analysis of computational performance, RGD 2012
W. Su et al, A Stable Runge-Kutta Discontinuous Galerkin Solver for Hypersonic Rarefied Gaseous Flows, RGD 2014.

RKDG for Boltzmann-ESBGK

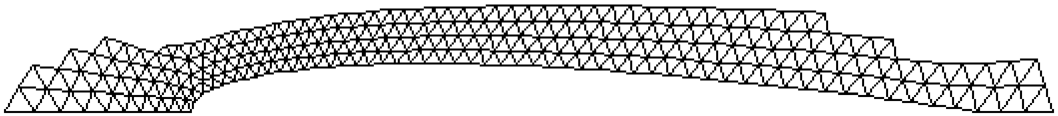

- In each triangle, solutions f_p^j are sought in the finite element space of discontinuous functions

$$f_p^j(t,x,y) = \sum_{l=1}^{k} F_{p,i}^{j,l}(t)\varphi_i^l(x,y)$$

- Basis Functions: supported in each triangle and dependent on the geometry
  - 2nd order: $\varphi_i^l(x,y) = a_0^l + a_1^l x + a_2^l y, \; l = 1,2,3$
  - 3rd other: $\varphi_i^l(x,y) = a_0^l + a_1^l x + a_2^l y + a_3^l x^2 + a_4^l y^2 + a_5^l xy, \; l = 1,2,..,6$
- Degree of freedom $F_{p,i}^{j,l}(t)$
  - Determined by the weak formulation of the governing system

$$\sum_{l=1}^{k} M_{ml}\frac{d}{dt}F_{p,i}^{j,l}(t) + \sum_{e\in\partial K_i}\int_e h_{e,K_i}(x,y,t)\varphi_i^m(x,y)d\Gamma - c_x^j\sum_{l=1}^{k}F_{p,i}^{j,l}Q_{ml}^x - c_y^j\sum_{l=1}^{k}F_{p,i}^{j,l}Q_{ml}^y$$

$$= \int_{K_i}\nu\,(f_{E,p}^j - \sum_{l=1}^{k}F_{p,i}^{j,l}\varphi_i^l(x,y))\varphi_i^m(x,y)dxdy \quad m = 1,\dots,k$$

- Time discretizations
  - Implicit Runge Kutta method up to 4th order

RKDG for Boltzmann-ESBGK

<u>Numerical Flux and Boundary Conditions:</u>

- The values of f_p^j are discontinuous at the edges. Two-point Lipschitz numerical fluxes are used to replace the real fluxes

$$h_{e,K_i}(x,y,t) = \begin{cases} \boldsymbol{c}^j \cdot \boldsymbol{n}_{e,K_i} f_p^j(int(K_i),t), & \boldsymbol{c}^j \cdot \boldsymbol{n}_{e,K_i} \geq 0 \\ \boldsymbol{c}^j \cdot \boldsymbol{n}_{e,K_i} f_p^j(ext(K_i),t), & \boldsymbol{c}^j \cdot \boldsymbol{n}_{e,K_i} < 0 \end{cases}$$

- The boundary values f_p^j *$(ext(K_i),t)$* should be specified at the boundary edges
  - symmetry boundary
  - specular-diffuse moving wall with give accommodation coefficient
  - periodic boundaries,
  - far pressure inlet/outlet boundaries
  - supersonic inlet/outlet boundaries

<u>Conservative Discretizations of the Collision Term:</u> $\nu\,(f_{E,p}^j - f_p^j)$

- Specify the equilibrium distribution equation
  - BGK model $f_{E,0}^j = \exp[a_1 - a_2(\boldsymbol{c}^j - \boldsymbol{u}) + a_3(c_x^j - u) + a_4(c_y^j - v)]$
  - ES-BGK model $f_{E,0}^j = \exp[a_1 - a_2(\vec{c}_x^{\,j} - u) + a_3(c_x^j - u) - a_4(c_y^j - v)^2 + a_5(c_y^j - v) + a_6 c_x^j c_y^j - a_7 c_y^{j2}]$
- In order to be consistent with the weak formulation of the DG method and to retain high order accuracy

$$a_s(x,y) = \sum_{l=1}^{k} A_s^l \varphi_i^l(x,y)$$

- the collision frequency and other macro properties can vary inside the spatial elements
- A_s^l obtained from the weak formulation of mass, momentum and energy conservation for the collision relaxations

RKDG: 1D Heat Transfer

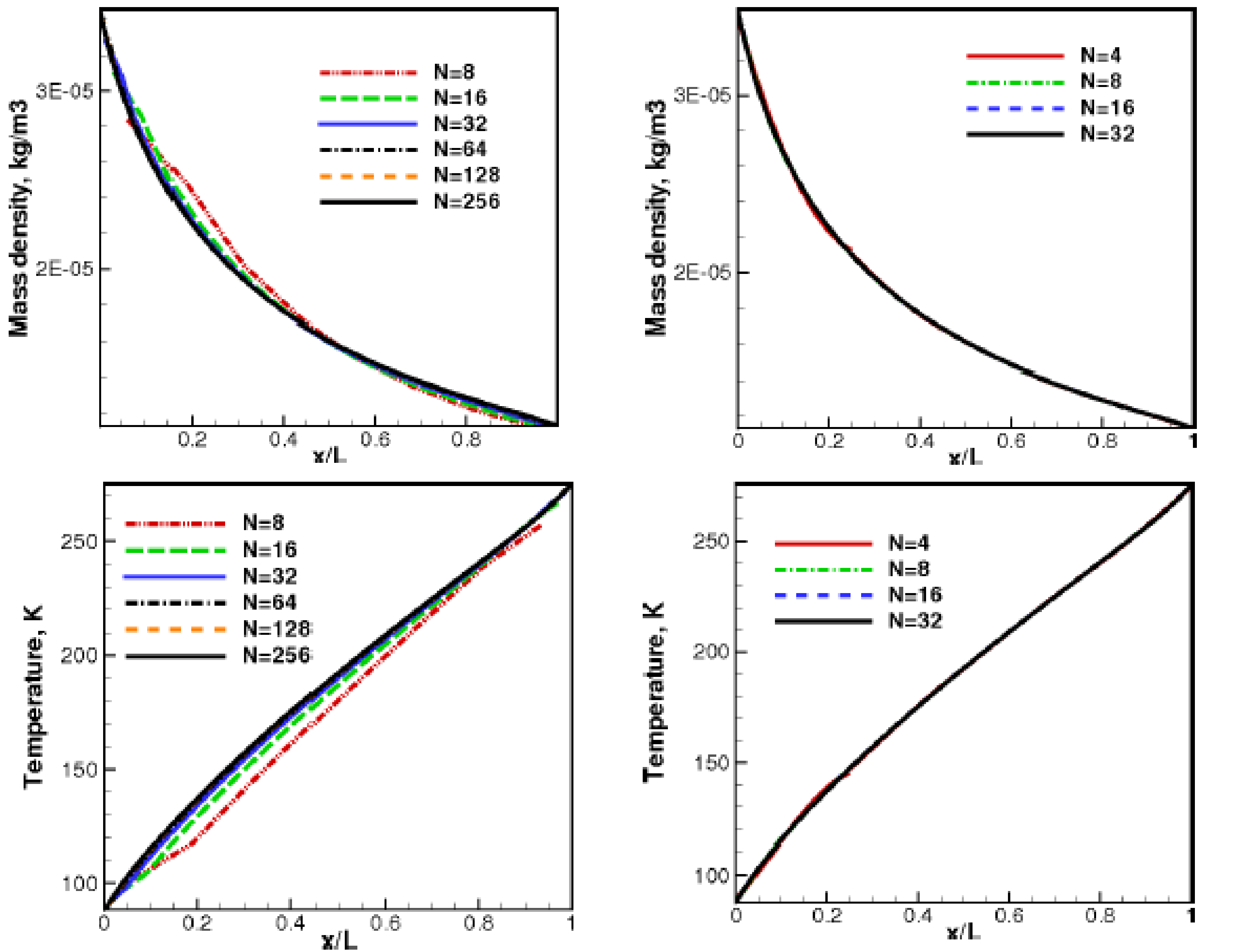

RKDG: 1D Heat Transfer

FVM-2

Case	CPU time, sec	$T(\frac{x}{L}=0.5)$, K
N=8	8.8E-002	180.532
N=16	0.388	187.241
N=32	1.62	190.526
N=64	6.54	191.847
N=128	25.86	192.305
N=256	107.1	192.447
N=512[1]	433.135	192.497

RKDG-3

Case	CPU time, sec	$T(\frac{x}{L}=0.5)$, K
N=4	2.47	192.142, 192.487
N=8	10.24	192.476, 192.511
N=16	45.24	192.5, 192.505
N=32	193.98	192.501, 192.502
N=64	784.08	192.5, 192.5

RKDG: 2D Heat Conduction

- 2D Conduction problem: *Kn*=0.0018 (comparison to analytical solution for heated lid cavity heat conduction)

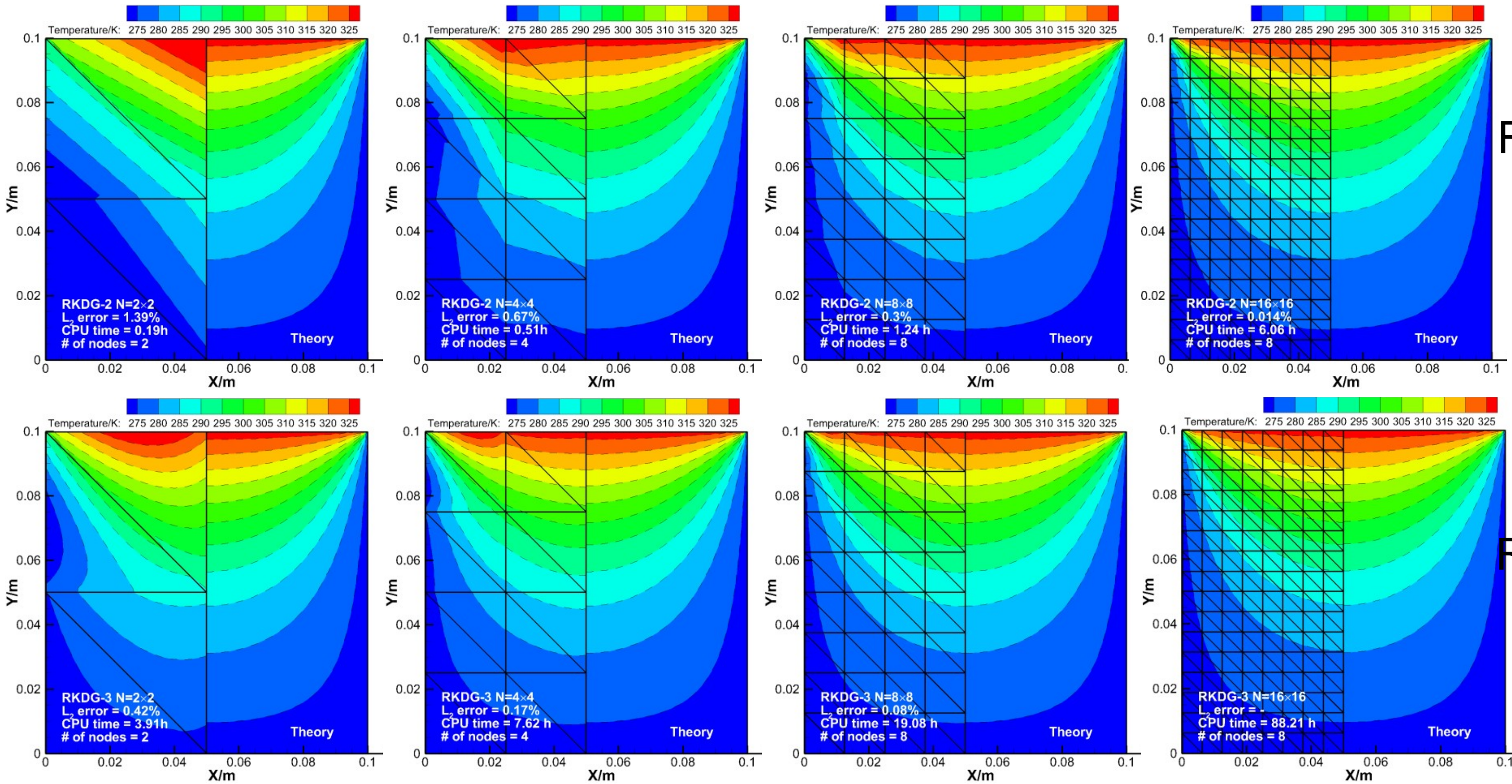

RKDG-2

RKDG-3

RKDG:2D flow around thermal actuator

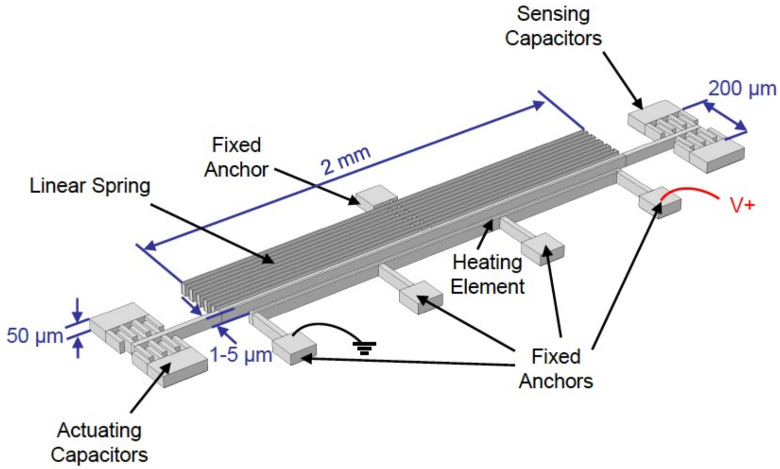

Parameter	Value
Initial Density	0.012 kg/m^3
Domain Width	400 [µm]
Domain Height	300 [µm]
Velocity Mesh	8x8x8
Gap	5 [µm]

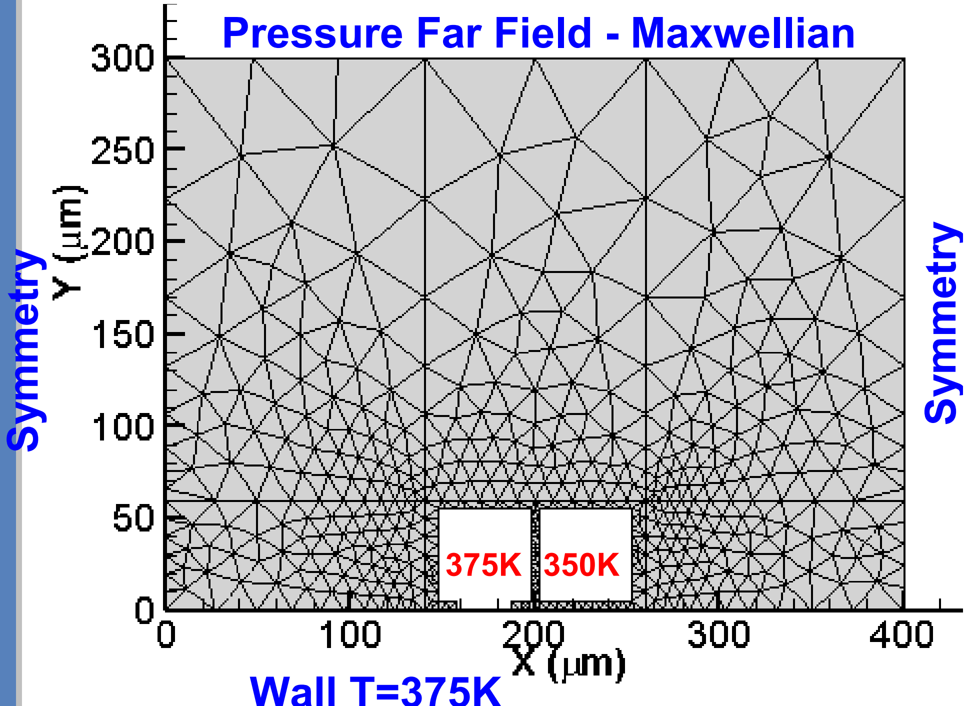

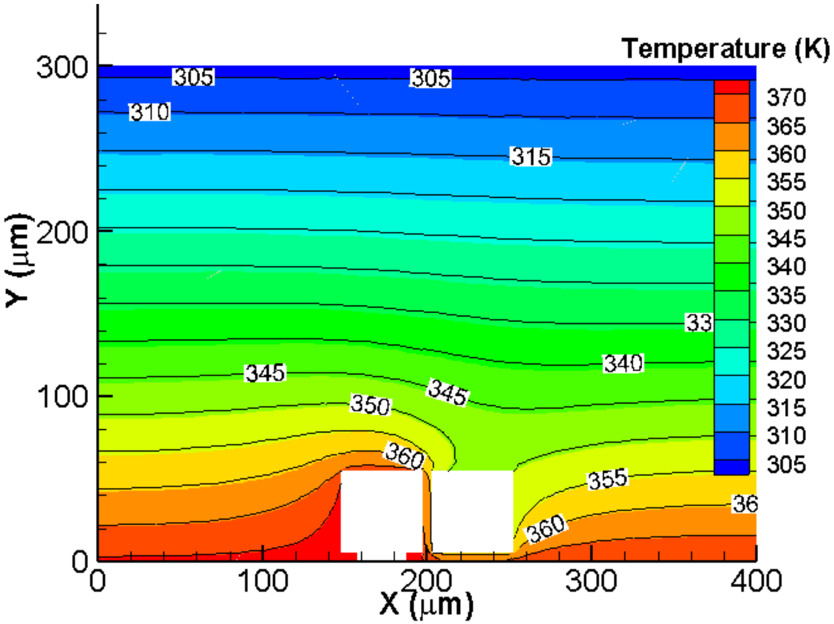

RKDG: Automatic Mesh Refinement

Coarse mesh in the lower gap
Max Face Error = 0.002

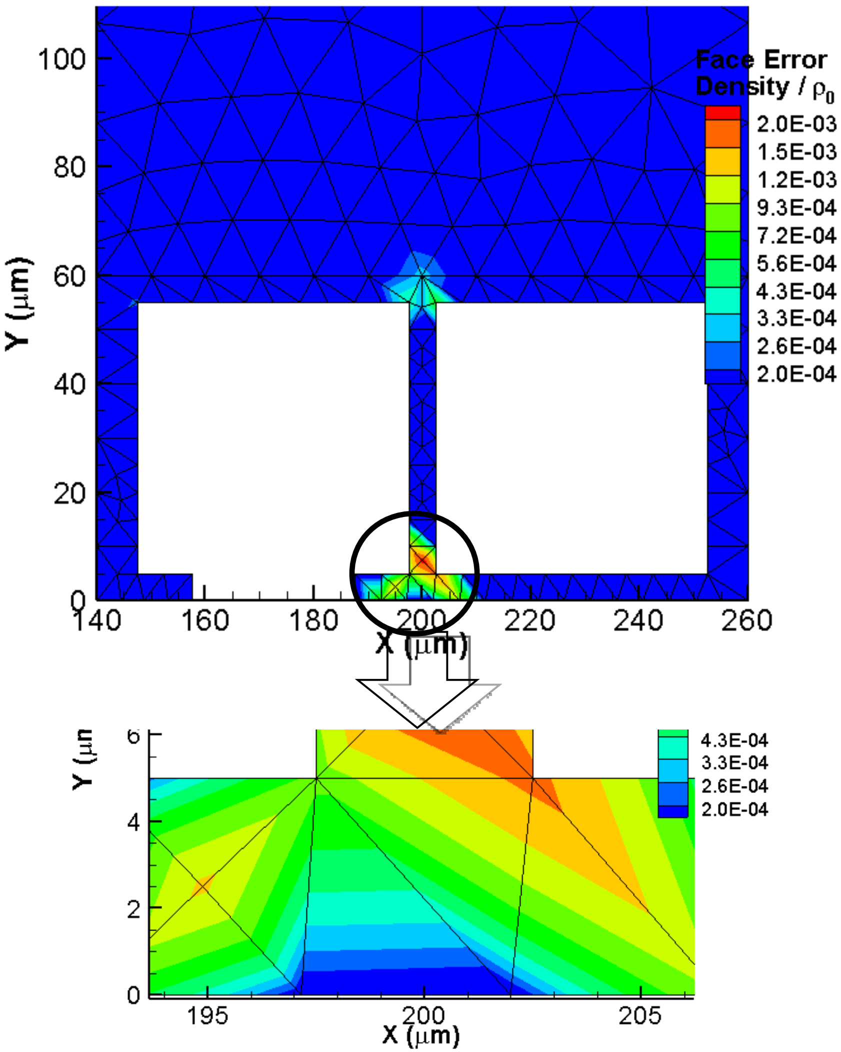

Refined mesh in the lower gap
Max Face Error = 0.0006

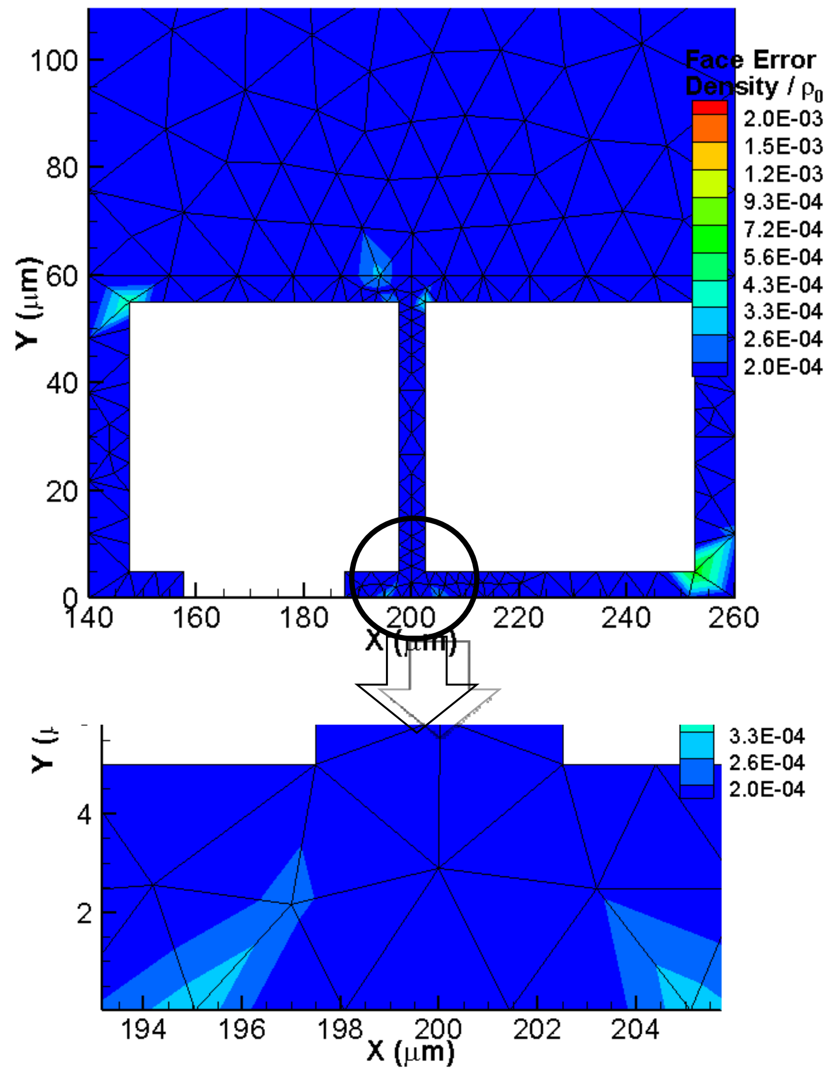

Exploiting Rarefied Flows for Novel Microdevices

Knudsen Thermal Force

Crookes' Radiometer
(Sir William Crookes, 1874)

$$U_{creep} \sim \lambda \cdot \frac{dT}{dx} = Kn \cdot \Delta T$$

Crookes Radiometer: Transverse

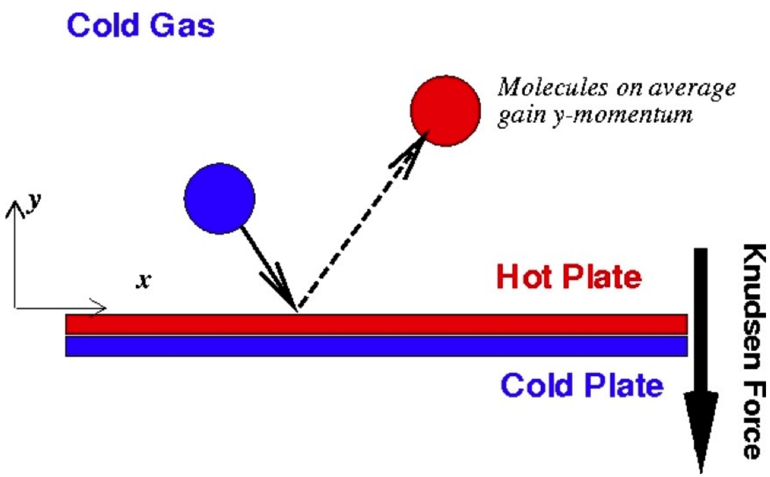

Knudsen Compressor: Longitudinal

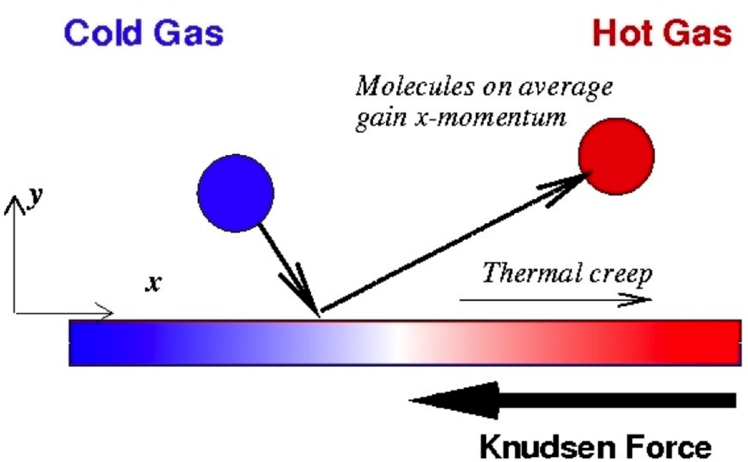

Kn force actuation

- Consequence of a thermal non-equilibrium between gas and solid
- Can be generated by resistive heating as well as optically Experimental data Passian et al, *PRL*, 2003 measurements using heated AFM probes

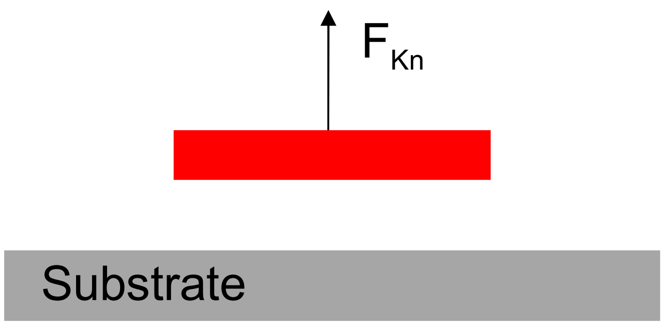

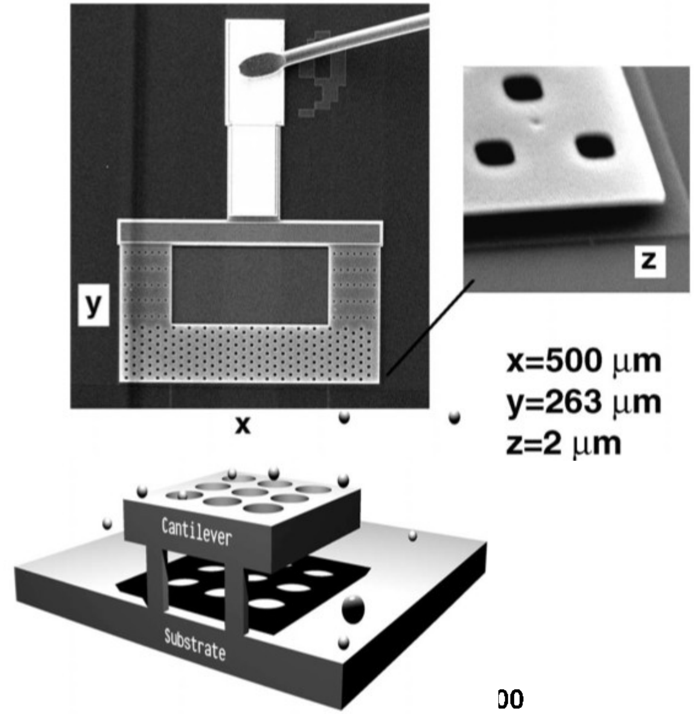

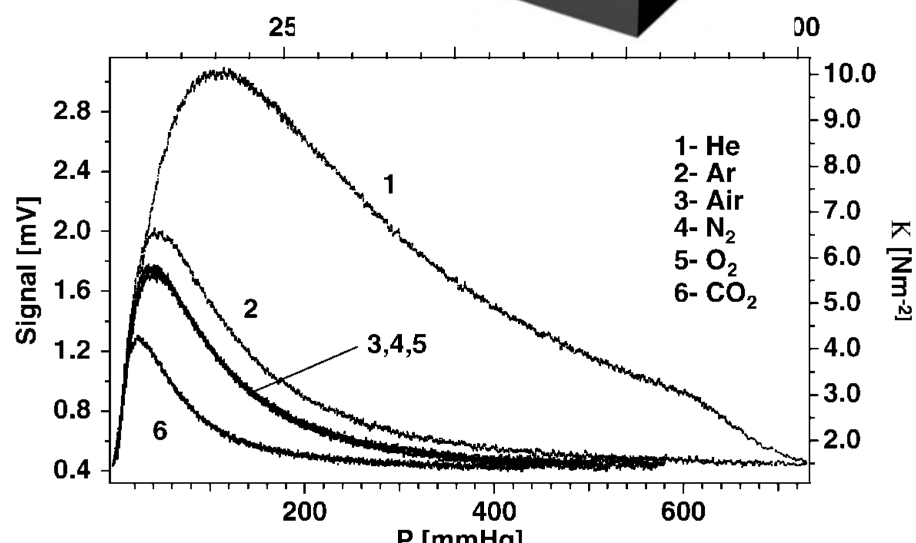

Passian et al data: Simulation Results

ESBGK simulations for planar geometry with equivalent front-to-side area ratio

- Velocity Contours and Streamlines:

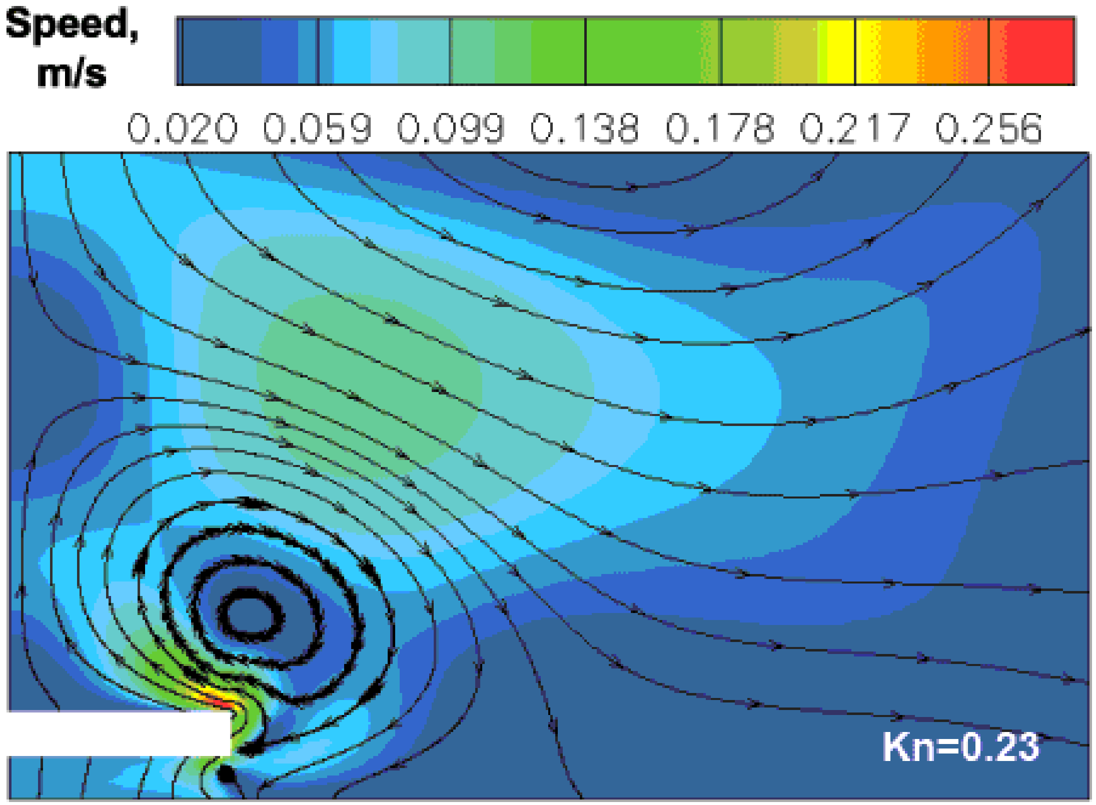

Experimental Validation

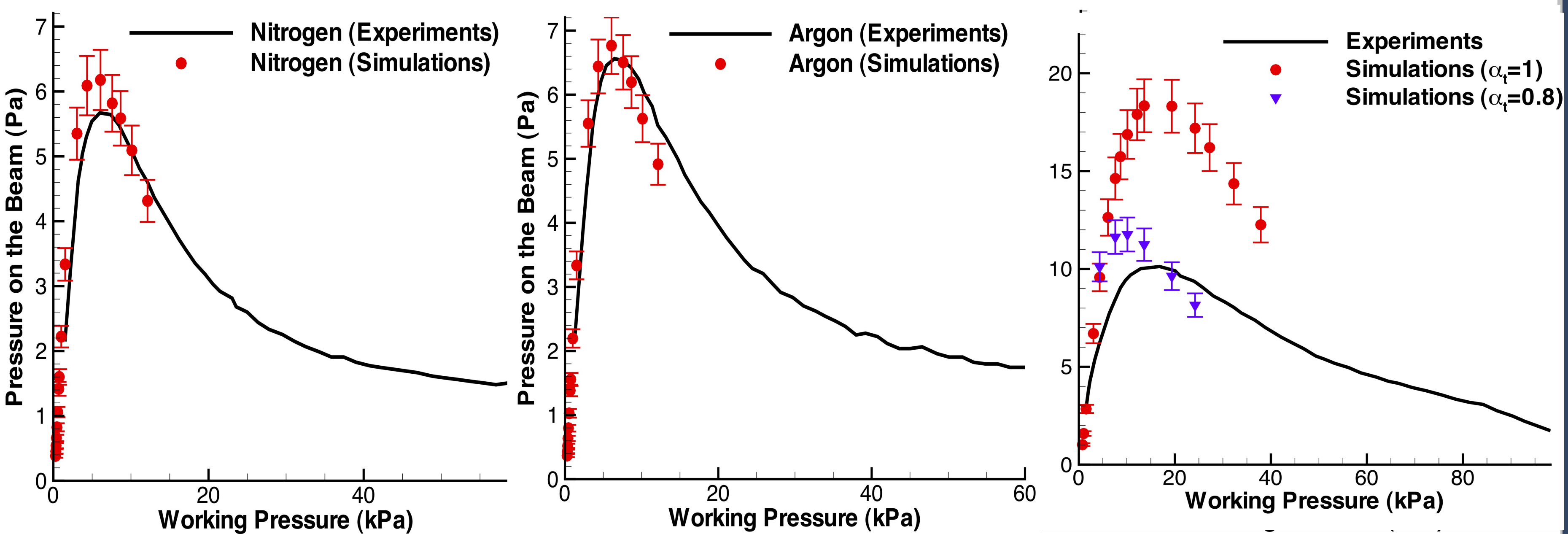

- Argon and Nitrogen simulations agree with experiments within 10%.
- Deviation for Helium is about 80% at the maximum of Knudsen force.

Nabeth, Chigullapalli, Alexeenko, *PRE*, 2011

Compact Model for Kn Force

Closed-form model for non-dimensional Knudsen thermal force coefficient for uniformly heated beam:

$$C_{Kn}\left(Kn,\frac{T}{\Delta T}\right) = \frac{F'}{w\rho R\Delta T} = \frac{1 + D\left(\frac{T}{\Delta T}\right)^{d} + E\left(\frac{T}{\Delta T}\right)^{e}}{AKn^{a} + BKn^{b} + CKn^{c}}$$

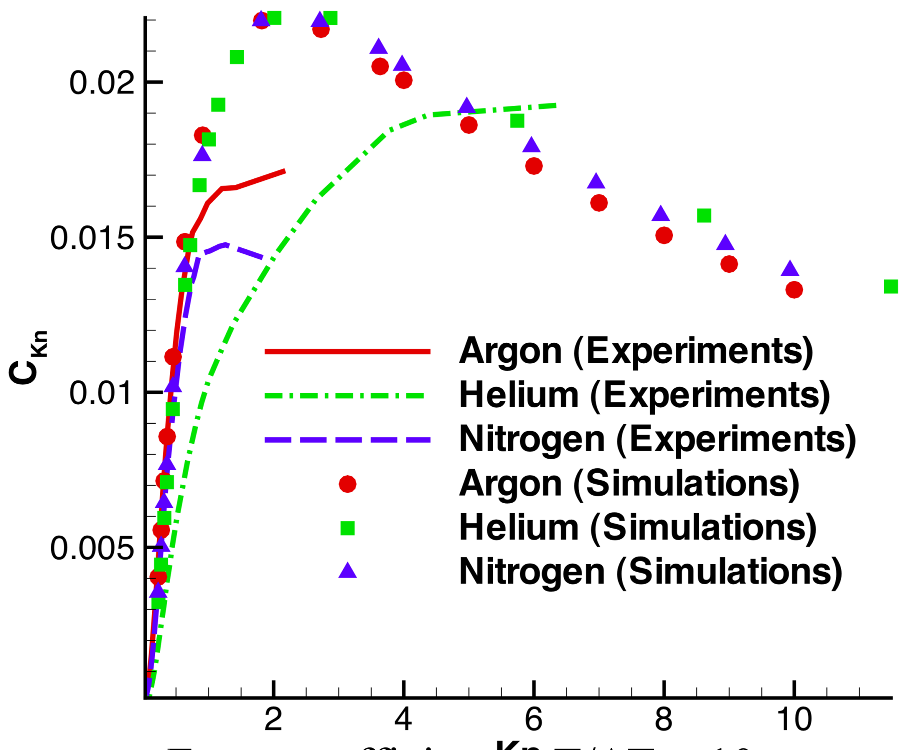

Force coefficient at T/ΔT = 10

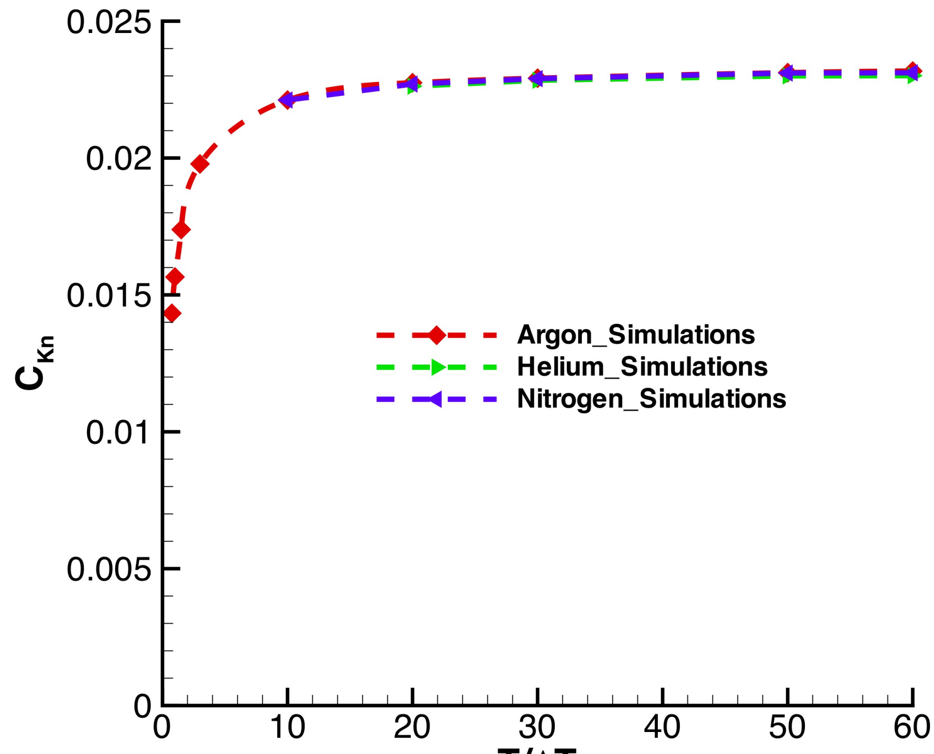

Force coefficient at Kn = 2

Force Enhancement and Reversal

- Uniformly heated beam (Passian et al, 2003)

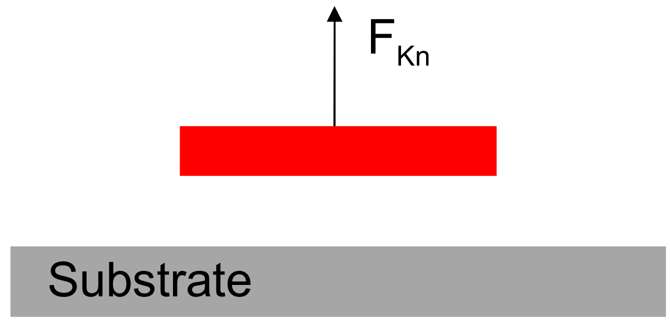

- Thermoelectric heating for bi-directional actuation (this work):

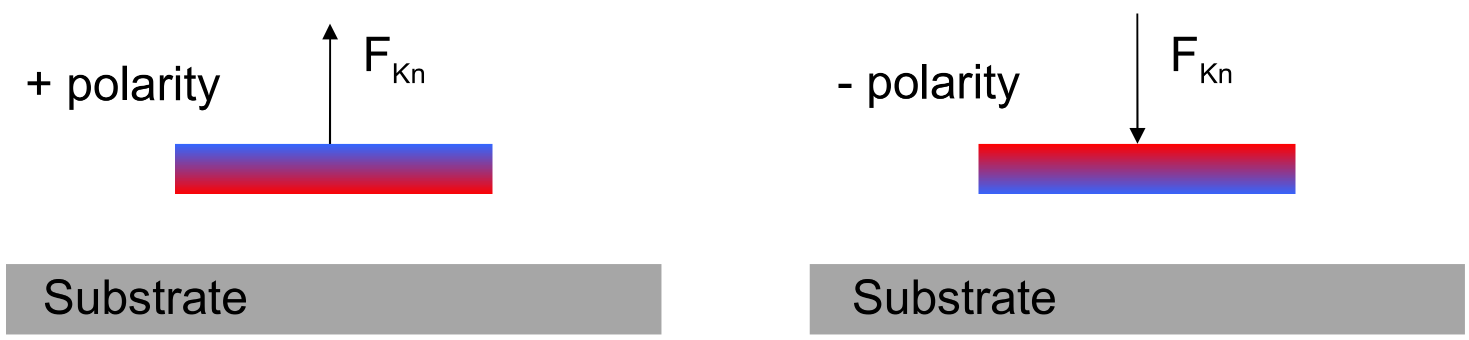

Modeling the Knudsen Force

Simulate Knudsen force on suspended heating element using ES-BGK model

- 2D-2V finite volume solver with second-order upwind fluxes
- 8th-order Gauss-Hermite quadrature in velocity space

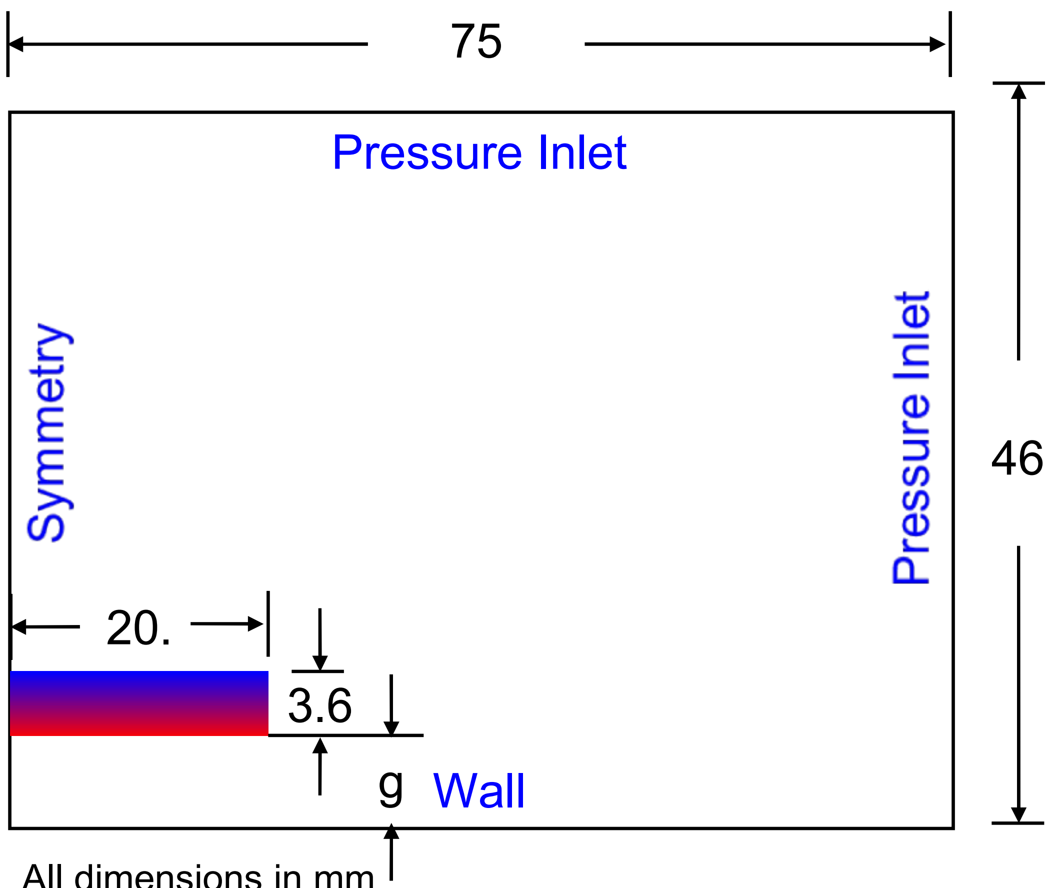

Parameter	Value
P_{ref}	298 – 12,522 Pa
$\lvert \Delta T_b \rvert$	25 K
$T_{b,mean}$	326 K
$T_{substrate}$	298 K
Parameter	**Value**

<u>Richardson Extrapolation:</u>
160x160 mesh for force within 2%

Simulation Results

Uniform Heating

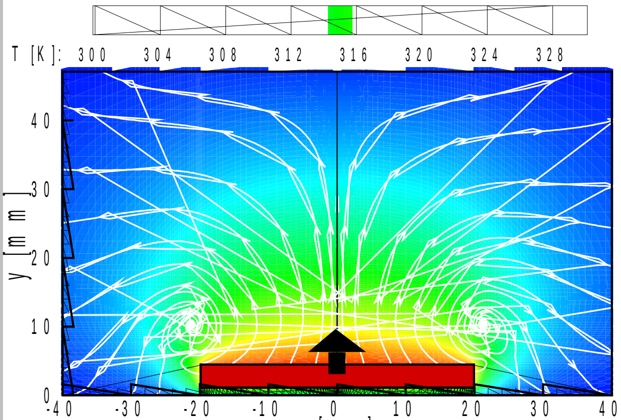

0.105% of p_0

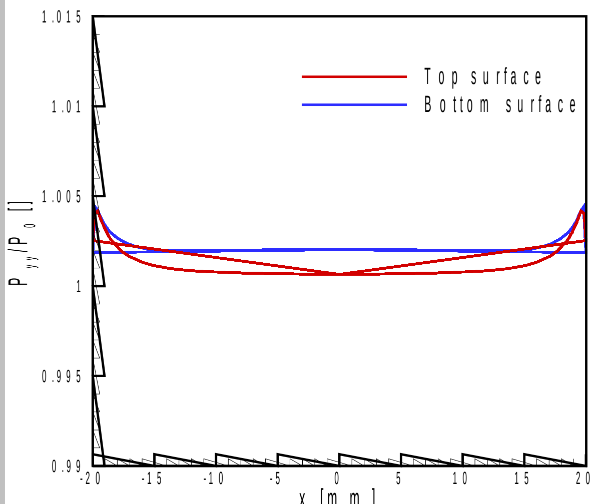

Thermoelectric: Bottom-Up

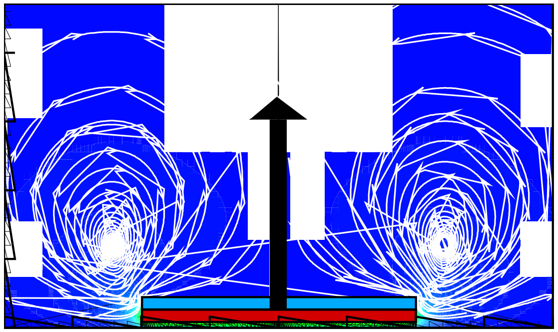

0.938% of p_0

X8.9 enhancement

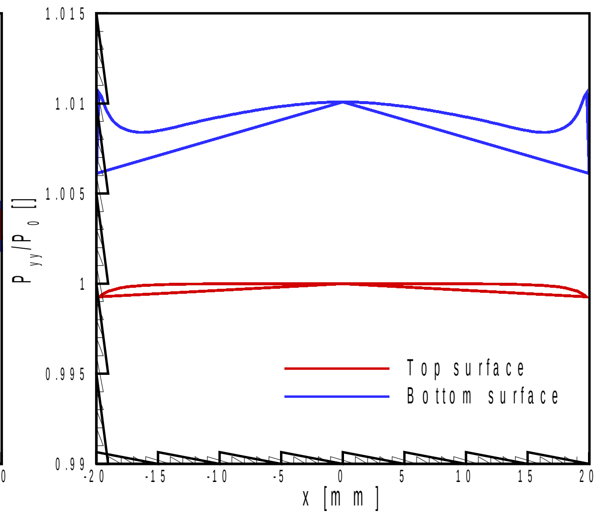

Thermoelectric: Top-Down

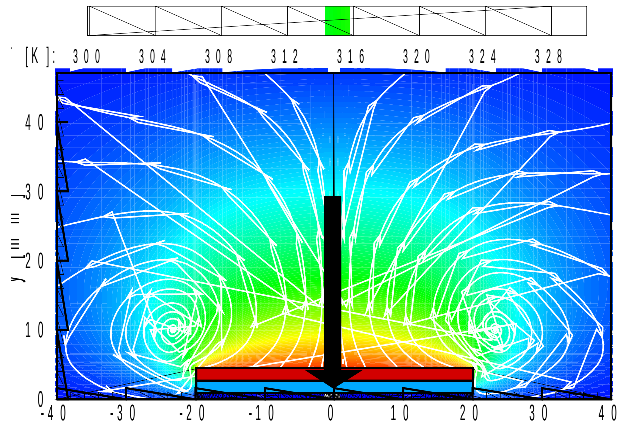

-0.557 % of p_0

X5.3 enhancement & reversal

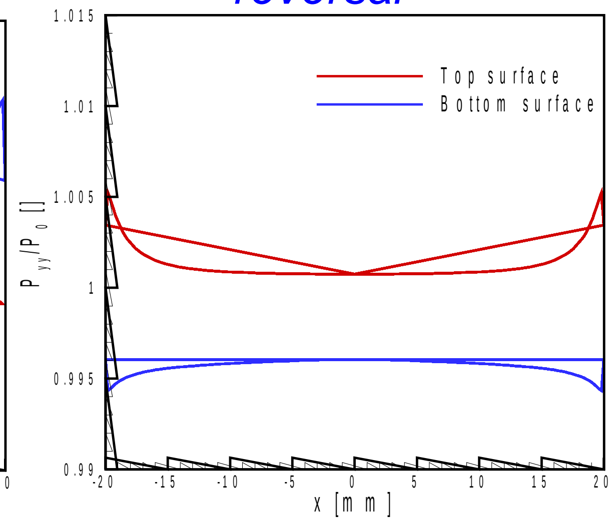

Experimental Setup

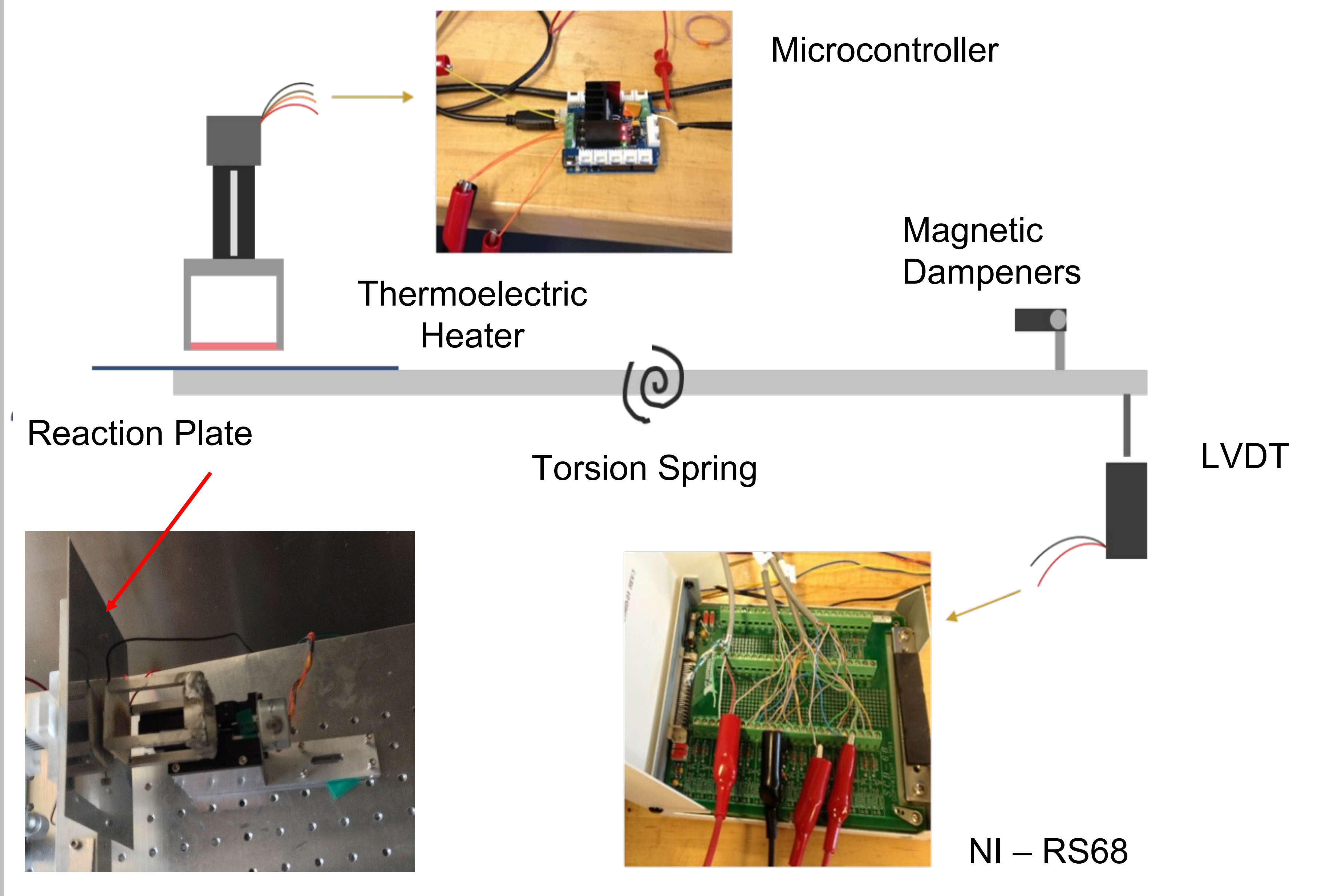

Experimental Setup

Purdue LEAP MicroNewton Thrust Stand

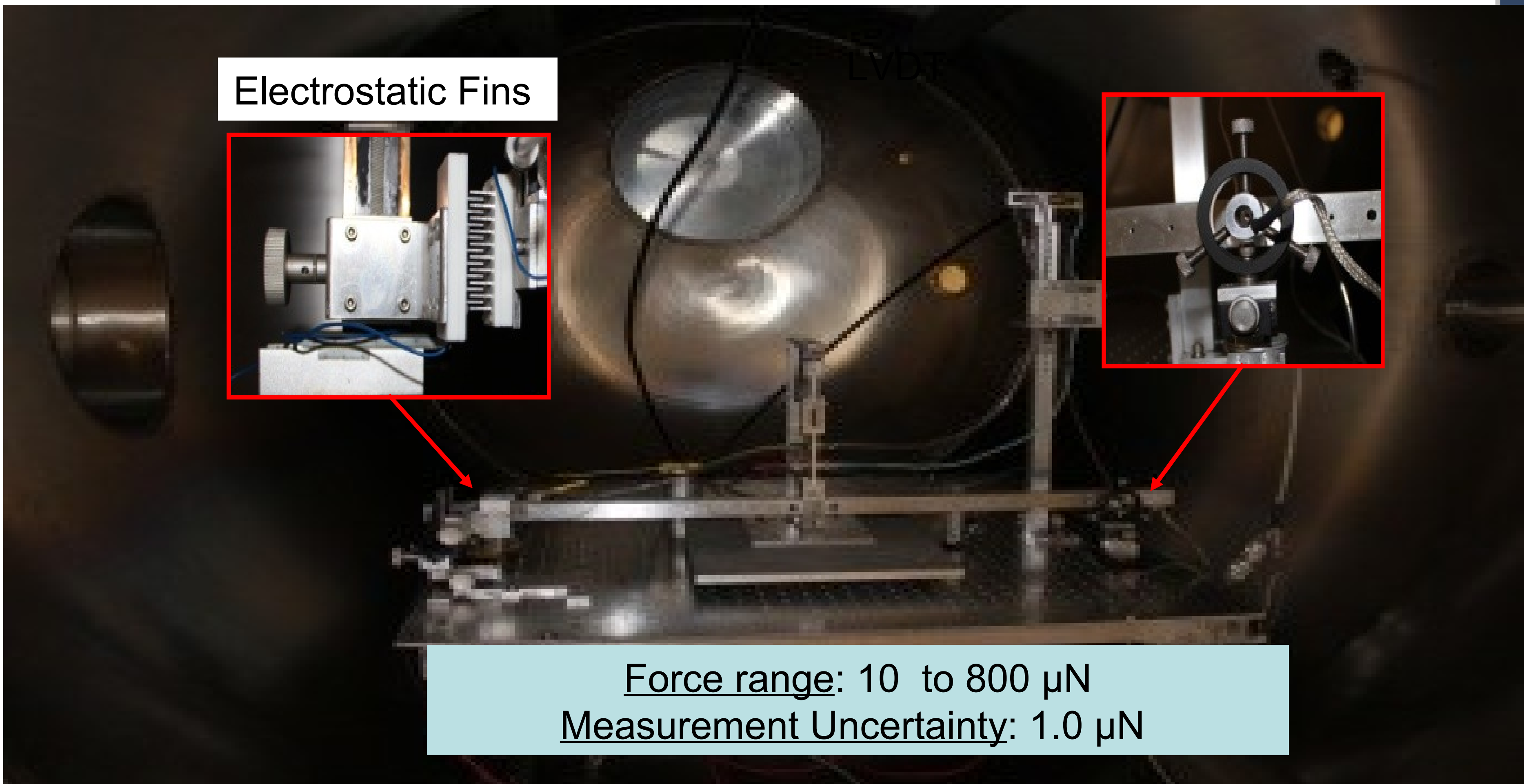

<u>Force range</u>: 10 to 800 μN
<u>Measurement Uncertainty</u>: 1.0 μN

Measurement Technique

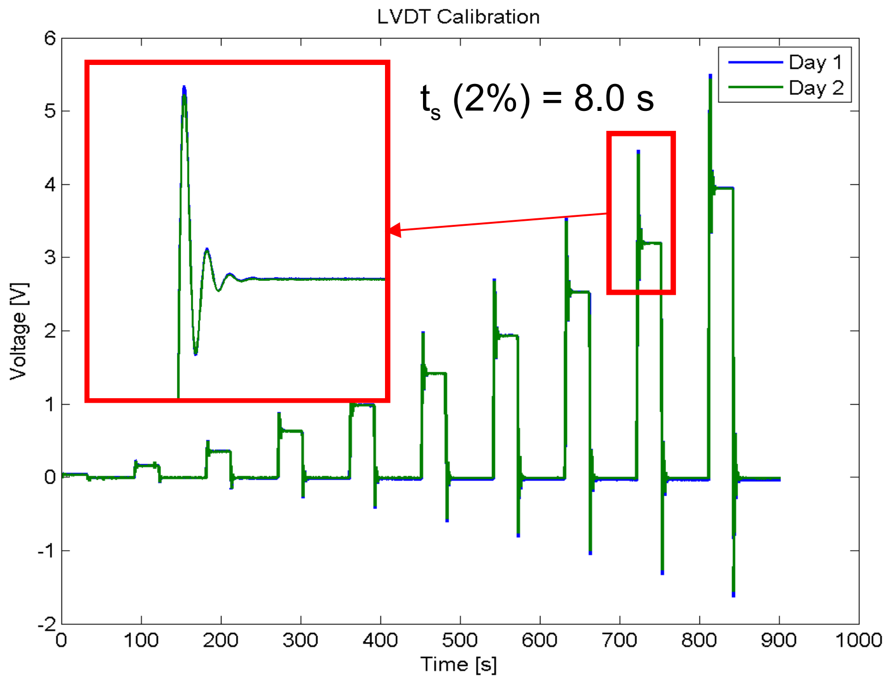

- Calibration performed at the beginning of each test day
- Sweep 0 - 100 V, 30 seconds high, 60 seconds low
  - Evaluate force from LVDT voltage

- Measure displacement of reaction plate
- Sweep 0.5 – 3.0 mm gap size at fixed pressure
  - Hold for 60 seconds to ensure steady state
  - Apply linear drift correction

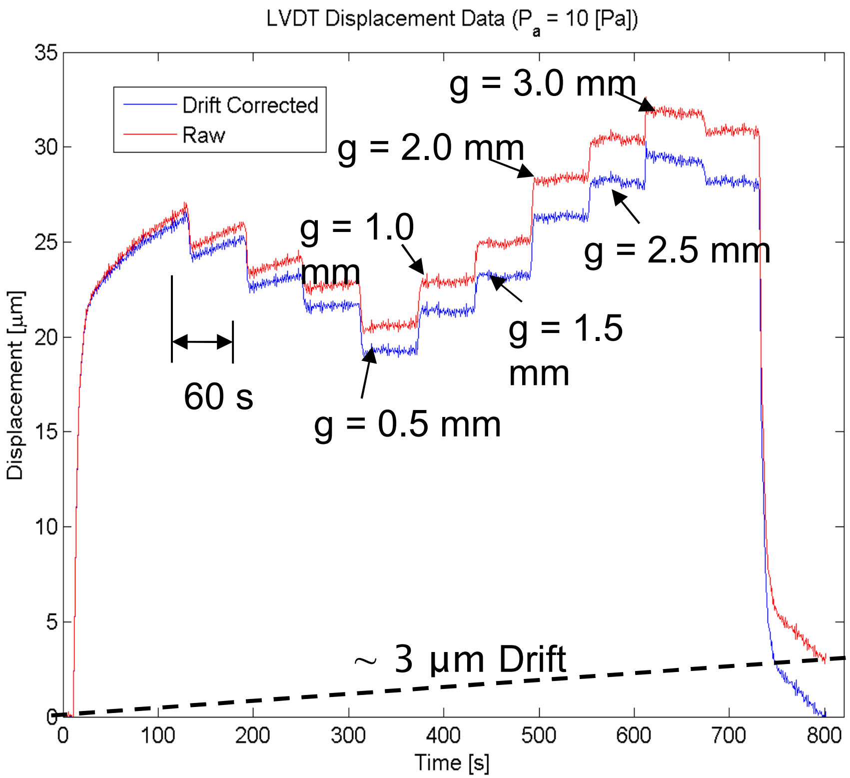

Comparison of Modeling and Experiment

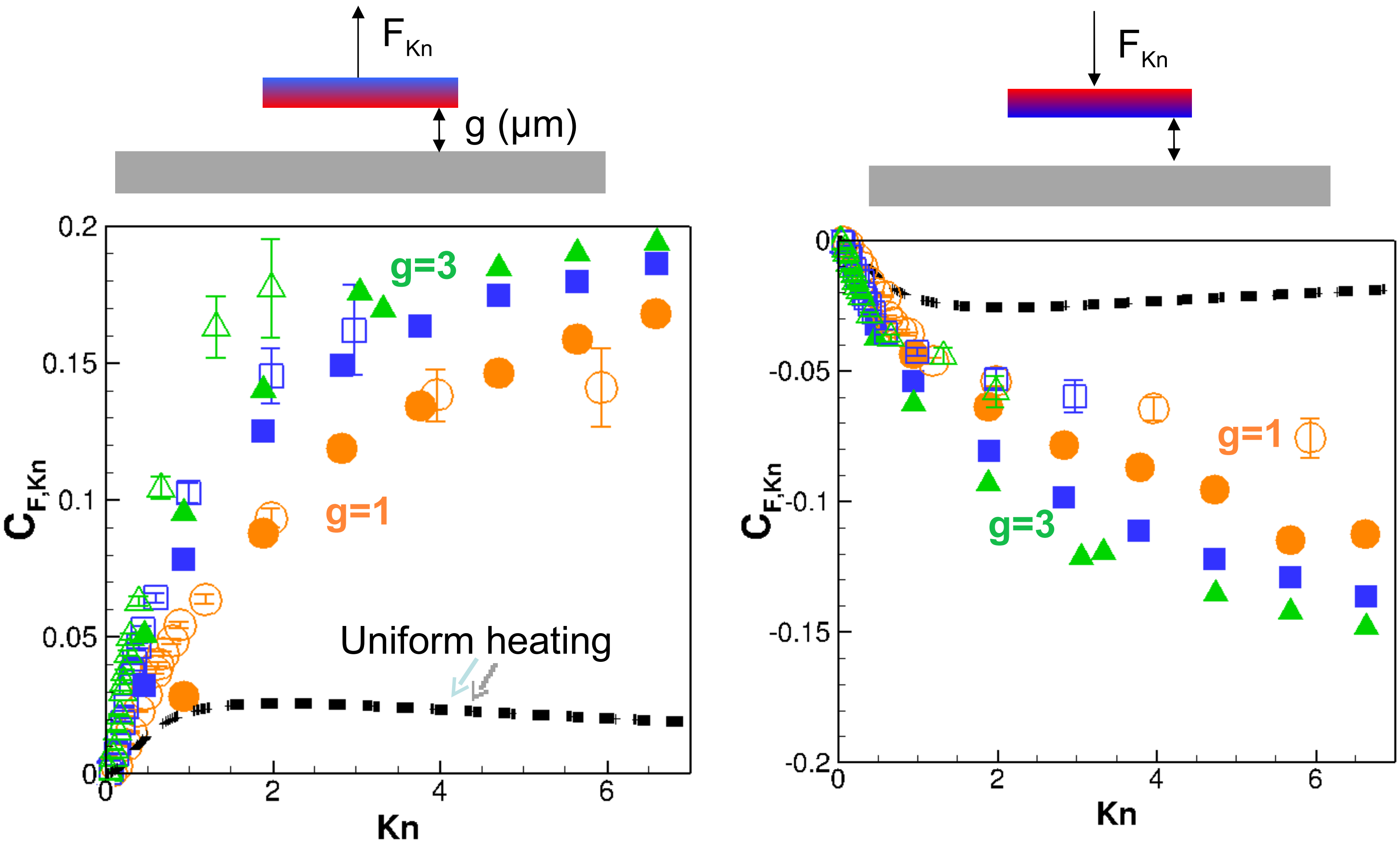

Maximum 36% error in $C_{F,Kn}$ between simulation and experiment

- Difference likely due to 3D effects in experimental measurements
- Errors likely stem from model inputs related to the heating element

Summary

New deterministic and stochastic kinetic approaches needed to explore and exploit significant new physics emerging at the micro/nanoscale:

- ❑ **Low-speed**
- ❑ **Moving geometries**
- ❑ **Coupling to structural/thermal/EM solvers**

Acknowledgements

- DOE NNSA Center for Predicting Reliability, Integrity and Survivability of Microsystems (PRISM)
- NSF "CAREER: Quantifying and Exploiting Knudsen Forces in Nano/Microsystems", CBET 1055453.